# Mcp1 and Mcp2, two novel proteins involved in mitochondrial lipid homeostasis

**Tao Tan[1], Cagakan Özbalci[2], Britta Brügger[2], Doron Rapaport[1,*] and Kai Stefan Dimmer[1,*]**

[1]Interfaculty Institute of Biochemistry, University of Tübingen, Hoppe-Seyler-Str. 4, 72076 Tübingen, Germany
[2]Heidelberg University Biochemistry Center, Im Neuenheimer Feld 328, 69120 Heidelberg, Germany
*Authors for correspondence (doron.rapaport@uni-tuebingen.de; kai-stefan.dimmer@uni-tuebingen.de)

*Accepted 21 May 2013*
*Journal of Cell Science 126, 3563–3574*

*doi: 10.1242/jcs.121244*

## Summary

The yeast mitochondrial outer membrane (MOM) protein Mdm10 is involved in at least three different processes: (1) association of mitochondria with the endoplasmic reticulum and mitochondrial lipid homeostasis (2) membrane assembly of MOM proteins, and (3) inheritance and morphogenesis of mitochondria. To decipher the precise role of Mdm10 in mitochondrial function, we screened for high-copy suppressors of the severe growth defect of the *mdm10*Δ mutant. We identified two novel mitochondrial proteins (open reading frames *YOR228c* and *YLR253w*) that we named Mdm10 complementing protein (Mcp) 1 and Mcp2. Overexpression of Mcp1 or Mcp2 restores the alterations in morphology and stability of respiratory chain complexes of mitochondria devoid of Mdm10, but the observed defect in assembly of MOM proteins is not rescued. Lipid analysis demonstrates that elevated levels of Mcp1 and Mcp2 restore the alterations in mitochondrial phospholipid and ergosterol homeostasis in cells lacking Mdm10. Collectively, this work identifies two novel proteins that play a role in mitochondrial lipid homeostasis and describes a role of Mdm10 in ergosterol trafficking.

**Key words:** Mitochondrial membranes, Lipid homeostasis, ERMES complex, Mdm10, *Saccharomyces cerevisiae*

## Introduction

Mitochondria are essential organelles of all eukaryotic cells that cannot form *de novo* and their biogenesis depends on different cellular processes. The vast majority of mitochondrial proteins have to be imported from the cytosol into the organelle. The proper inheritance of mitochondria into the daughter cell is facilitated by the tubular morphology of the organelle and its interaction with cytoskeletal structures. Furthermore, the intimate contact of mitochondria with the ER plays an important, although still ill-defined, role in mitochondrial function. A central function of the ER–mitochondria contact sites is probably lipid exchange between the two compartments (for reviews, see Daum and Vance, 1997; Rowland and Voeltz, 2012).

Mdm10 is a yeast mitochondrial protein proposed to be involved in many mitochondrial processes. It was first described in 1994 and shown to be an integral mitochondrial outer membrane (MOM) protein. Mutation and deletion of the gene results in altered mitochondrial morphology (condensed giant organelles) and distribution phenotype (Sogo and Yaffe, 1994). Deletion of the genes encoding the MOM proteins Mdm12, Mmm2/Mdm34 and the ER protein Mmm1 led to similar growth defects and mitochondrial inheritance and morphology phenotypes (Burgess et al., 1994; Berger et al., 1997; Dimmer et al., 2002; Youngman et al., 2004; Kornmann et al., 2009). Therefore these components were referred to as tubulation mediators (Okamoto and Shaw, 2005). Additionally it was reported that Mmm1 and Mdm10 are involved in the interaction of mitochondria with the actin cytoskeleton (Boldogh et al., 1998). Moreover, Mmm1, Mdm10 and Mdm12 have been identified as components of a high molecular mass complex essential for the efficient transmission of mtDNA to the daughter cell (Boldogh et al., 2003). Mdm10 is predicted to be a β-barrel protein of the outer membrane of mitochondria and depends on the topogenesis of the mitochondrial outer membrane β-barrel proteins (TOB) complex [also known as sorting and assembly machinery (SAM) complex] for proper insertion into the MOM (Paschen et al., 2003; Wiedemann et al., 2003). In addition, Mdm10 was reported to be a transient component of the TOB complex and to play a role in the assembly of β-barrel proteins (Meisinger et al., 2004; Wideman et al., 2010; Yamano et al., 2010b).

Recently, Mdm10 and the other tubulation mediators (Mdm12, Mmm1 and Mmm2) were shown to be components of the so called ER–mitochondria encounter structure (ERMES) complex (Kornmann et al., 2009). The MOM calcium-binding rho GTPase Gem1 was also suggested to associate with the ERMES complex (Kornmann et al., 2011; Stroud et al., 2011), although this notion was very recently debated (Nguyen et al., 2012). Accumulating evidence suggests that the ERMES complex and its component Mdm10 are involved in the lipid homeostasis of mitochondria. Mitochondria lacking Mdm10 have altered cardiolipin (CL) and phosphatidylethanolamine (PE) levels (Kornmann et al., 2009; Osman et al., 2009; Yamano et al., 2010b; Nguyen et al., 2012; Tamura et al., 2012a). Collectively, the aforementioned putative roles of Mdm10 leave open the question what the primary function of this protein is.

In the current study, we investigated the distinct role of Mdm10. To this end, we screened for multi-copy suppressors of the *mdm10*Δ growth phenotype and identified two proteins of so far unknown function, Mcp1 and Mcp2. Our results demonstrate that these novel mitochondrial proteins play a role in mitochondrial lipid homeostasis and further shed new light on the involvement of the ERMES complex in ergosterol trafficking.

Journal of Cell Science

## Results

### Mcp1 and Mcp2 are high-copy suppressors of *mdm10*Δ

The deletion of *MDM10* leads to reduced growth of yeast cells under all conditions tested (Sogo and Yaffe, 1994). Most prominent is the growth defect on non-fermentable carbon sources (Fig. 1A). To better understand the molecular function of Mdm10 we searched for new components genetically interacting with Mdm10. Thus, we screened for high-copy suppressors of the *mdm10*Δ growth phenotype. To avoid indirect effects, we confirmed that the used haploid *mdm10*Δ strain still contained mtDNA ($\rho^+$, data not shown). We transformed *mdm10*Δ cells with a yeast genomic library cloned in a high copy number (2 μ based) yeast shuttle vector. Transformants were initially selected on selective medium and then replica plated on glycerol-containing rich medium. Suppressor clones were identified by growth at elevated temperatures (37℃) and then analysed again at normal and reduced temperatures. We screened a total of 30,000 colonies and identified five clones that exhibited prominent rescue of the growth phenotype at 37℃.

Next, plasmids isolated from these clones, and a plasmid encoding *MDM10* as a control, were transformed into the *mdm10*Δ cells and the growth of the transformed cells was monitored at both 30℃ and 37℃ on a non-fermentable carbon source. In addition, the inserted DNA fragments in the rescuing plasmids were sequenced. Two of the clones contained the *MDM10* open reading frame (ORF) (Fig. 1A, #18, and data not shown). Two other plasmids contained a DNA fragment encoding *ARS1523*, *YOR228C* and *WTM2* as annotated sequence features (Fig. 1A, #15, and data not shown). *ARS1523* is an autonomously replicating sequence, whereas *WTM2* encodes a transcriptional modulator without apparent link to mitochondrial function. *YOR228C* encodes an uncharacterized protein that was found in a proteomic analysis of the yeast mitochondrial outer membrane (Zahedi et al., 2006). The fifth clone contained a plasmid that comprised the annotated elements *SYM1*, *YLR252W*, *YLR253W* and *NDL1* (Fig. 1A, #13). Interestingly, plasmid #13 has a very weak rescue capacity at 37℃, but rescues the growth defect quite well at 30℃ (Fig. 1A). According to the Saccharomyces Genome Database (SGD) (www.yeastgenome.org), *NDL1* has no obvious connection to mitochondrial function, and *YLR252W* is a dubious ORF. *SYM1* encodes for a transporter of the inner mitochondrial membrane (Trott and Morano, 2004; Dallabona et al., 2010; Reinhold et al., 2012) with no obvious link to Mdm10 or any of its proposed functions. Of note, *YLR253W* encodes for a yet uncharacterized protein that was detected in the mitochondrial proteome (Reinders et al., 2006).

We concentrated on the two non-characterized ORFs *YOR228C* and *YLR253W* as well as *SYM1* and cloned them into a centromeric yeast expression vector. Overexpression of both former proteins rescued the growth phenotype of *mdm10*Δ cells under almost all tested conditions while *YOR228C* was under all conditions the more effective suppressor (Fig. 1B; supplementary material Fig. S1). We therefore named the proteins Mcp1 (Mdm10 complementing protein 1, Yor228c) and Mcp2 (Mdm10 complementing protein 2, Ylr253w). In contrast, overexpression of Sym1 could not restore the growth phenotype of *mdm10Δ* cells (supplementary material Fig. S2). Of note, overexpression of both Mcp1 and Mcp2 failed to rescue the *mdm10*Δ growth defect at extreme conditions such as high temperature and non-fermentable carbon source (37℃ and YPG medium; supplementary material Fig. S1A).

To test whether the rescue effects of Mcp1 and Mcp2 are additive we co-overexpressed both proteins in the *mdm10Δ* strain. However, overexpression of both proteins did not result in any additional rescue effects beyond those observed with Mcp1 alone (supplementary material Fig. S3).

Mdm10 is part of the ERMES complex that contains also the mitochondrial proteins Mdm12 and Mmm2 as well as the ER

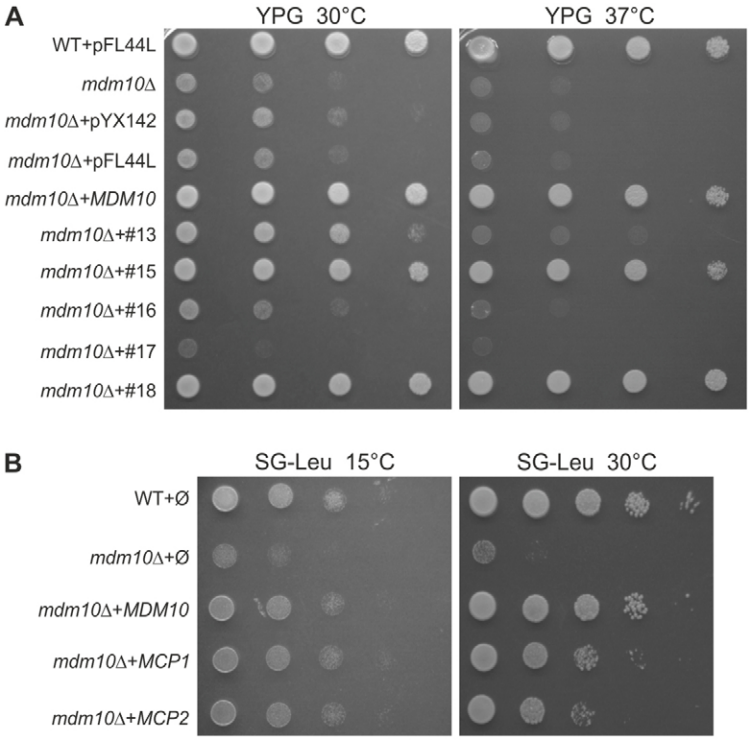


**Fig. 1. Mcp1 and Mcp2 are multi-copy suppressors of *mdm10Δ*.** (**A**) Wild-type or *mdm10*Δ cells were transformed with the empty plasmids pFL44L and pYX142 or with plasmids of the genomic library isolated from positive candidates of the screen (#10, 13, 15–18). Cells were grown to an $OD_{600}$ of 1.0 and spotted on a YPG plate directly and in a 1:5 dilution series. Plasmid #15 contains *YOR228C* (*MCP1*), #13 contains *YLR253W* (*MCP2*) and #18 contains *MDM10*. (**B**) Overexpression of Mcp1 and Mcp2 rescues the growth defect of *mdm10*Δ cells. Wild-type cells transformed with the empty plasmid pYX142 (Ø) or *mdm*10Δ cells containing the empty plasmid (Ø) or a plasmid encoding Mcp1, Mcp2 or Mdm10 as a control were analysed by drop dilution assay at 15℃ or 30℃ on synthetic medium containing glycerol (SG). All dilutions are in fivefold increments.

protein Mmm1. In contrast to the suppression capacity of Mcp1 and Mcp2, overexpression of the other ERMES components Mmm1, Mmm2 or Mdm12 did not rescue the growth phenotype of *mdm10*Δ cells (supplementary material Fig. S4). These results suggest that the primary function of Mcp1 and Mcp2 differs from those of the ERMES components.

### Mcp1 and Mcp2 are mitochondrial membrane proteins

We were next interested in the subcellular localization of Mcp1 and Mcp2. Previous high-throughput studies suggest that both are mitochondrial proteins (Huh et al., 2003; Reinders et al., 2006; Zahedi et al., 2006). However, we wanted to study the localization and topology of both proteins on a single gene level. To this end we expressed C-terminally HA-tagged plasmid-borne constructs of both proteins in the corresponding deletion strain as well as a genomically FLAG-tagged version of Mcp2. The HA-tagged proteins were confirmed to be functional as their overexpression complemented the *mdm10Δ* growth phenotype (supplementary material Fig. S5).

Cells expressing either Mcp1–HA or Mcp2–HA were fractionated by differential centrifugation into mitochondrial, microsomal and cytosolic fractions. Both Mcp1–HA and Mcp2–HA were present in the mitochondrial fraction (Fig. 2A,B). Similar behaviour was observed with a genomically FLAG-tagged version of Mcp2 (supplementary material Fig. S6A). Mcp1 is a protein of 303 amino acid residues, with five predicted α-helical transmembrane domains (TMDs) (http://www.cbs.dtu.dk/services/TMHMM/). Homologue proteins of Mcp1 could be found only in fungi (http://blast.ncbi.nlm.nih.gov/Blast.cgi). The primary sequence of Mcp2 comprises 569 amino acids, and in contrast to Mcp1, a homologue could be found in all higher eukaryotes. The human orthologue is called aarF domain containing kinase 1 (ADCK-1). Comparison of the sequences of Mcp2 and ADCK-1 shows 33% identity with coverage of 92% (http://blast.ncbi.nlm.nih.gov/Blast.cgi). Several prediction programs suggest at least one TMD within the primary sequence of Mcp2 (Biegert et al., 2006).

To study, whether Mcp1 and Mcp2 are indeed integral membrane proteins, we subjected mitochondria containing Mcp1–HA or Mcp2–HA to an alkaline extraction treatment. Under these conditions, soluble and peripheral membrane proteins can be separated by centrifugation from integral membrane proteins. Mcp1–HA (Fig. 2C), Mcp2–HA (Fig. 2D), and the genomically tagged Mcp2–FLAG (supplementary material Fig. S6B) were found, like the integral outer membrane protein Tom70 or Porin, in the pellet fraction, suggesting that both Mcps are integral membrane proteins.

Since mitochondria have two distinct membranes, we wanted to know in which one Mcp1 and Mcp2 are located. To that end, we treated mitochondria containing HA-tagged Mcps with proteinase K (PK) under different conditions. Mcp1–HA full length protein was no longer detected after the proteolytic treatment of intact organelles and instead, two fragments of around 15 kDa were observed (Fig. 2E). As expected for a MOM protein, the amount of these fragments was reduced if mitochondria were swollen and the outer membrane was ruptured before protease treatment. Furthermore, solubilisation of the membrane by the detergent Triton X-100 exposed Mcp1 to complete degradation (Fig. 2E). Hence, we propose that Mcp1 is a MOM protein, with its C-terminus facing the intermembrane space (IMS). This proposal is in agreement with previous

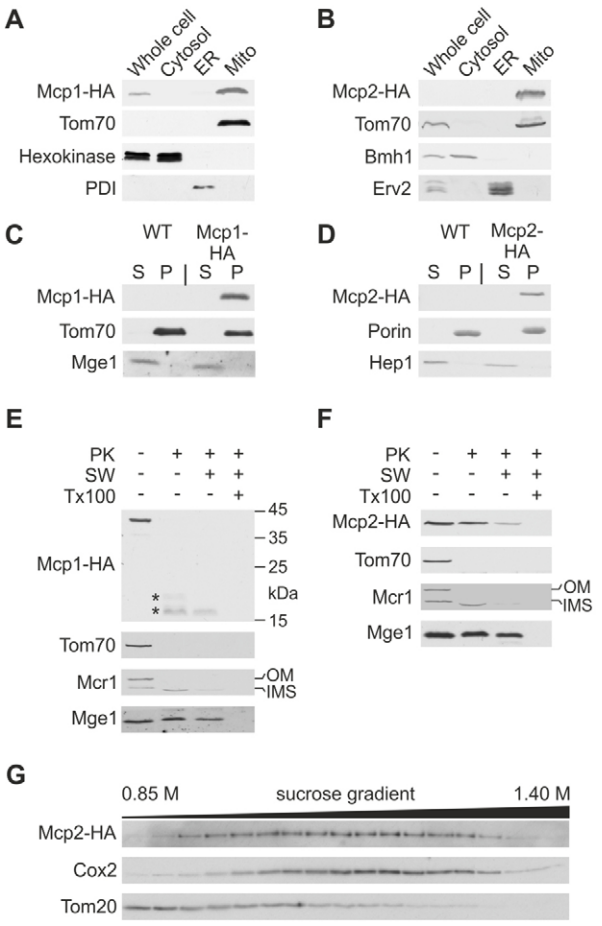


**Fig. 2. Subcellular and submitochondrial localization of Mcp1 and Mcp2.** (**A**,**B**) Mcp1 and Mcp2 are mitochondrial proteins. Whole cell lysate (Whole cell) and cytosol, light microsomal (ER) and mitochondrial (Mito) fractions of cells expressing either Mcp1–HA (A) or Mcp2–HA (B) were analysed by SDS-PAGE and immunodecoration with antibodies against the HA tag, the mitochondrial protein Tom70, a marker protein for the cytosol (hexokinase or Bmh1) and an ER marker protein (disulfide isomerase, PDI or Erv2). (**C**,**D**) Mcp1 and Mcp2 are membrane proteins. Mitochondria isolated from wild-type, Mcp1–HA (C)- or Mcp2–HA (D)-expressing cells were subjected to alkaline extraction. The supernatant (S) and pellet (P) fractions were analysed by SDS-PAGE and immunodecoration with antibodies against the indicated proteins: Tom70 and Porin, integral MOM proteins; Mge1 and Hep1, soluble matrix proteins. (**E**) Mcp1 is a MOM protein. Mitochondria isolated from cells expressing Mcp1–HA were treated with proteinase K (PK) under different conditions. Mitochondria were kept intact, the MOM was ruptured by hypo-osmolar swelling (SW), or mitochondria were lysed completely by the addition of the detergent Triton X-100 (Tx100). Samples were precipitated with TCA and analysed by SDS-PAGE and immunodecoration with antibodies against the HA tag, or the indicated mitochondrial proteins. Proteolytic fragments are marked with an asterisk. Tom70 is a MOM protein exposed to the cytosol; Mcr1 is a dually located mitochondrial protein with an isoform in the MOM and another in the intermembrane space (IMS) (Hahne et al., 1994); Mge1 is a soluble matrix protein. (**F**) Mcp2 is protected from protease digestion and is degraded upon rupture of the outer membrane. Mitochondria isolated from cells expressing Mcp2–HA were treated and analysed as described in E. (**G**) Mcp2 behaves like an inner membrane protein in density gradient centrifugation. Mitochondrial vesicles obtained by swelling and sonication of mitochondria isolated from cells expressing Mcp2–HA were subjected to sucrose density gradient centrifugation. Fractions of the gradient were collected and analysed by SDS-PAGE and immunodecoration with antibodies against the indicated proteins: Cox2, an integral protein of the MIM; Tom20, an integral MOM protein.

identification of Mcp1 in the MOM proteome (Zahedi et al., 2006). In contrast to Mcp1, Mcp2–HA was protected from the protease as long as the MOM was intact. If the outer membrane was ruptured by hypo-osmolar treatment, the protein was partially degraded by the protease (Fig. 2F). These results suggest that Mcp2 is a mitochondrial membrane protein exposed to the IMS located either in the inner or outer membrane. To discriminate between these two possibilities, we separated inner and outer membrane mitochondrial vesicles by density gradient centrifugation. Analysis of the different fractions of the gradient showed that Mcp2–HA migrated similar to the inner membrane protein Cox2, whereas as expected, the integral MOM protein Tom20 was found in fractions with lower density (Fig. 2G). These findings suggest that Mcp2 is an integral protein of the mitochondrial inner membrane.

### Alterations in the levels of Mcp1 and Mcp2 do not influence the growth of yeast cells

To better understand the importance of the two novel proteins for cellular functions, we investigated whether the deletion of Mcp1, Mcp2 or both results in growth phenotypes of yeast cells. All three deletion mutants grew similarly to wild-type cells under all tested conditions (Fig. 3A and data not shown). We next tested the outcome of overexpression of either Mcp1 or Mcp2 and did not observe any effect on the growth behaviour of wild-type yeast cells (Fig. 3B and data not shown). Taken together it appears that both proteins are not essential for optimal cellular growth under the investigated conditions.

### Mcp1 and Mcp2 rescue the mitochondrial morphology phenotype of *mdm10*Δ cells

To decipher the molecular function of Mcp1 and Mcp2 we first analysed mitochondrial morphology upon their deletion. To visualize the mitochondria, we transformed the cells of interest with a plasmid encoding matrix targeted GFP (mtGFP) (Westermann and Neupert, 2000). Cells lacking Mcp1 or Mcp2 did not show alterations in mitochondrial morphology (Fig. 4A,B). We further asked whether overexpression of Mcp1 or Mcp2 could restore the *mdm10*Δ morphology phenotype. To this end we co-transformed the *mdm10*Δ strain with an mtRFP plasmid together with overexpression plasmids encoding either Mcp1 or Mcp2. Overexpression of Mcp1 in the *mdm10*Δ strain resulted in a rescue of the morphology phenotype to the same extent as re-introducing Mdm10 itself (Fig. 4C,D). In contrast, only about 20% of the *mdm10Δ* cells overexpressing Mcp2 harboured restored tubular networks and about 40% of the cells exhibited a variable morphology phenotype ranging from elongated condensed structures to short tubules (Fig. 4C,D). To better understand the role of Mcp1 and Mcp2 in mitochondrial morphology we overexpressed the proteins also in wild-type cells. Increased levels of Mcp1 had no effect on the organelle's morphology, yet overexpression of Mcp2 resulted in shortened, condensed or aggregated mitochondria in some of the cells (Fig. 4E,F). Collectively, it appears that elevated levels of Mcp2 affect the morphogenesis of mitochondria.

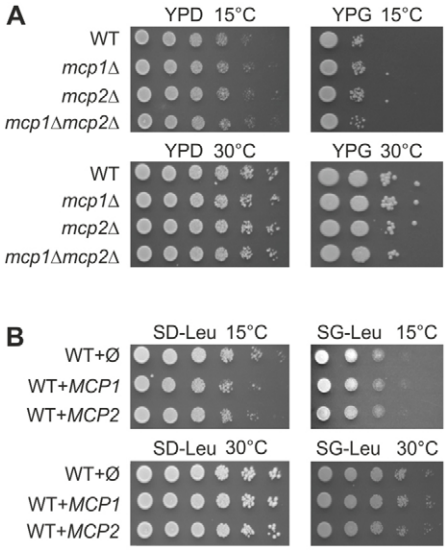


**Fig. 3. Growth of yeast cells is not affected by alterations in Mcp1 and Mcp2 levels.** (**A**) Cells of the indicated deletion strains and wild-type cells were analysed by drop dilution assay on YPD or YPG medium at the indicated temperatures. (**B**) Wild-type cells transformed with the empty plasmid pYX142 (Ø) or a plasmid encoding either Mcp1 or Mcp2 were analysed at the indicated temperatures by drop dilution assay on synthetic medium lacking leucine containing either glucose (SD-Leu) or glycerol (SG-Leu).

### Mcp1 and Mcp2 have no effect on the steady state levels of mitochondrial proteins

It was reported that mitochondria lacking Mdm10 show also a mild reduction in the levels of subunit Tom22 of the translocase of the outer membrane (TOM) complex (Meisinger et al., 2004). We wanted to know whether the observed growth rescue by overexpression of Mcp1 or Mcp2 could be due to restored Tom22 levels or due to elevated levels of other mitochondrial proteins. To address this question, we isolated mitochondria from wild-type or *mdm10*Δ cells bearing an empty plasmid or from *mdm10*Δ cells overexpressing Mcp1, Mcp2 or Mdm10 itself. In contrast to the report above we were not able to detect reduced levels of Tom22 in mitochondria lacking Mdm10. Unaffected Tom22 levels were observed in both crude mitochondria (Fig. 5A) and mitochondria purified by a Percoll gradient (data not shown). A potential explanation for this discrepancy is the different genetic background of the deletion strains. Whereas we used the wild-type background W303, Meisinger et al. (Meisinger et al., 2004) utilized the BY4741/2/3 background. Indeed, it was recently reported that steady state levels of TOM and TOB components vary between *mdm10*Δ mutants of different genetic backgrounds (Yamano et al., 2010b). Nonetheless, we did not observe substantial changes in the steady state levels of the other TOM components Tom20, Tom40 or Tom70 as well as of the TOB subunits Mas37 and Tob55 upon overexpression of Mcp1 or Mcp2 in *mdm10*Δ cells or in cells lacking Mdm10 (Fig. 5A and data not shown). Taken together, it seems that the suppression capacity of Mcp1 and Mcp2 is not related to alteration in the levels of import components of the MOM.

### Mcp1 and Mcp2 do not play a direct role in the assembly of TOM and TOB complexes

A major consequence of loss of Mdm10 is an altered assembly of TOM and TOB complexes as reflected by blue native PAGE (BN-PAGE) analysis (Meisinger et al., 2004; Yamano et al., 2010b). Absence of Mdm10 leads to reduced levels of the assembled TOM complex and to an additional unassembled species of Tom40 of about 100 kDa (Fig. 5B, second lane)

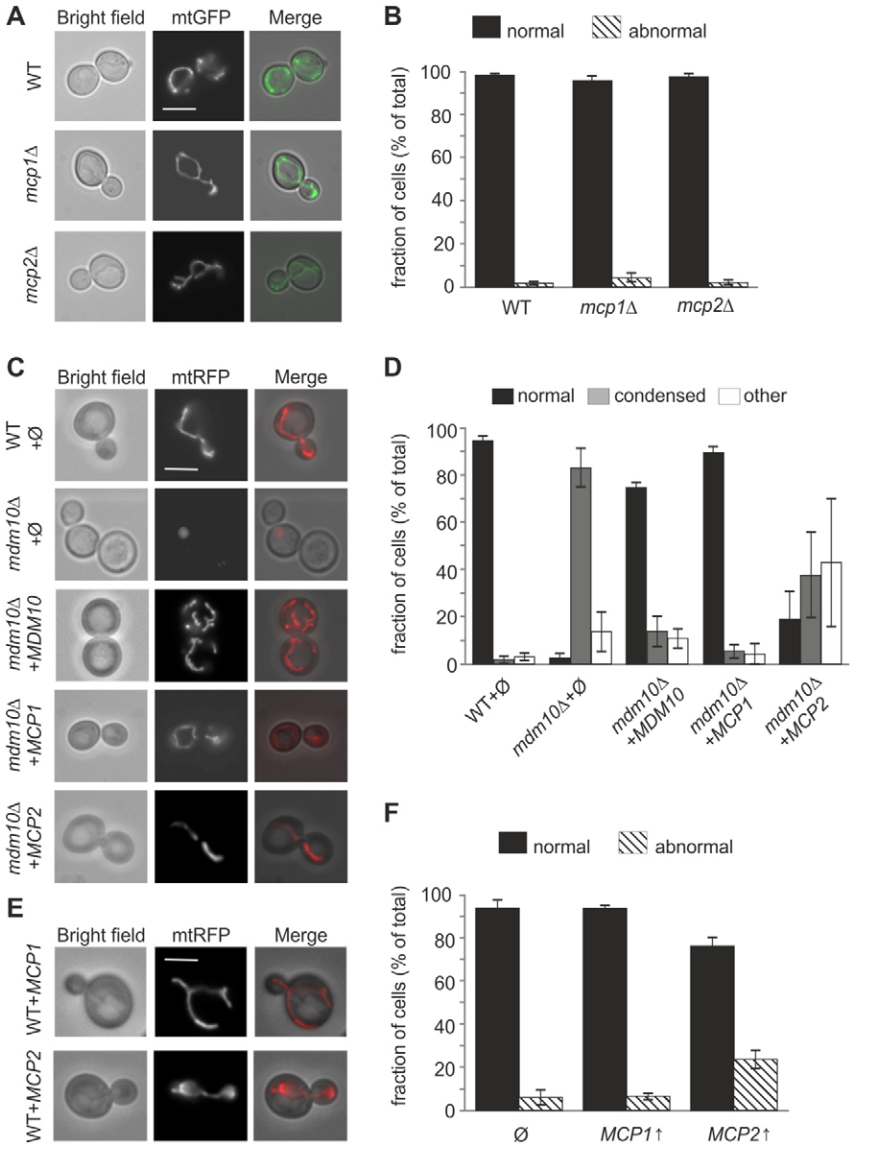


**Fig. 4. Mcp1 and Mcp2 can affect mitochondrial morphogenesis.** (**A**) Loss of Mcp1 or Mcp2 has no influence on mitochondrial morphology. Wild-type, *mcp1Δ* or *mcp2Δ* cells expressing mitochondrially targeted GFP (mtGFP) were analysed by fluorescence microscopy. Typical images of the three different strains are shown (scale bar: 5 µm). (**B**) Analysis of the cells described in A. Average values with standard deviation bars of three independent experiments with at least $n=100$ cells in each experiment are shown. (**C**) Overexpression of Mcp1 and Mcp2 rescues the mitochondrial morphology defect in *mdm10Δ* cells. Wild-type and *mdm10Δ* cells expressing mitochondrially targeted RFP (mtRFP) were transformed with an empty plasmid (Ø) or a plasmid expressing Mdm10, Mcp1 or Mcp2. Cells were analysed by fluorescence microscopy. Typical images of the five different strains are shown (scale bar: 5 µm). (**D**) Analysis of the cells described in C. The average percentages with standard deviation bars of three independent experiments with at least $n=100$ cells in each experiment are shown. (**E**) Overexpression of Mcp2 but not Mcp1 leads to alterations of the tubular mitochondrial network. Wild-type cells expressing mitochondrially targeted RFP (mtRFP) were transformed with a plasmid overexpressing either Mcp1 or Mcp2. Cells were grown to mid-logarithmic phase on synthetic medium to select for both plasmids and then analysed by fluorescence microscopy. Typical images of the two different strains are shown (scale bar: 5 µm). (**F**) Analysis of the cells described in E. The average percentages with standard deviation bars of three independent experiments with at least $n=100$ cells in each experiment are shown.

(Meisinger et al., 2004; Yamano et al., 2010b). Upon re-introduction of Mdm10 in *mdm10*Δ cells this lower molecular mass complex is no longer observable. In contrast, upon overexpression of Mcp1 or Mcp2 the unassembled species is still visible and TOM complex levels are mildly reduced (Fig. 5B). We therefore conclude that the rescue by Mcp1 and Mcp2 is not derived by an effect on the stability of the TOM complex.

We next wondered whether Mcp1 and Mcp2 play a role in the efficiency of TOM complex assembly. Previous reports showed that in the absence of Mdm10 the typical assembly pathway of radiolabeled newly imported Tom40 via the 250 kDa intermediate I and the 100 kDa intermediate II is hampered (Model et al., 2001; Meisinger et al., 2004; Yamano et al., 2010b). We made the same observation in *mdm10*Δ mitochondria isolated from the W303 genetic background (Fig. 5C). In the absence of Mdm10 only a minor portion of the radiolabeled Tom40 molecules became assembled after 90 minutes of *in vitro* import (Fig. 5C). To test whether Mcp1 or Mcp2 could restore this defect, we used mitochondria isolated from an *mdm10*Δ strain overexpressing Mcp1 or Mcp2. Although we could see a slight increase in the amount of assembly intermediates I and II upon overexpression of either Mcp1 or Mcp2, this overexpression did not affect the amount of assembled TOM complex (Fig. 5C). We therefore propose that Mcp1 and Mcp2 do not take over the role of Mdm10 in the assembly of functional TOM holo-complex. The increase in assembly intermediates could be a secondary effect of the not completely restored mitochondrial lipid composition (see below).

Mitochondria lacking Mdm10 show also a defect in the *in vitro* import of Tom22 and a 400 kDa assembly intermediate is observed under these conditions (Meisinger et al., 2004). Mitochondria lacking Mdm10 with elevated levels of either Mcp1 or Mcp2 exhibited only a slight restoration, if at all, in this assembly defect (Fig. 5D). Of note, we observed an increase in the overall amount of newly synthesized Tom22 molecules incorporated into mitochondria lacking Mdm10 and overexpressing Mcp2. However, we could not find any support for a direct role of Mcp2 in the import of Tom22. These results substantiate our aforementioned findings that Mcp1 and Mcp2 have no direct function in the assembly of the TOM complex.

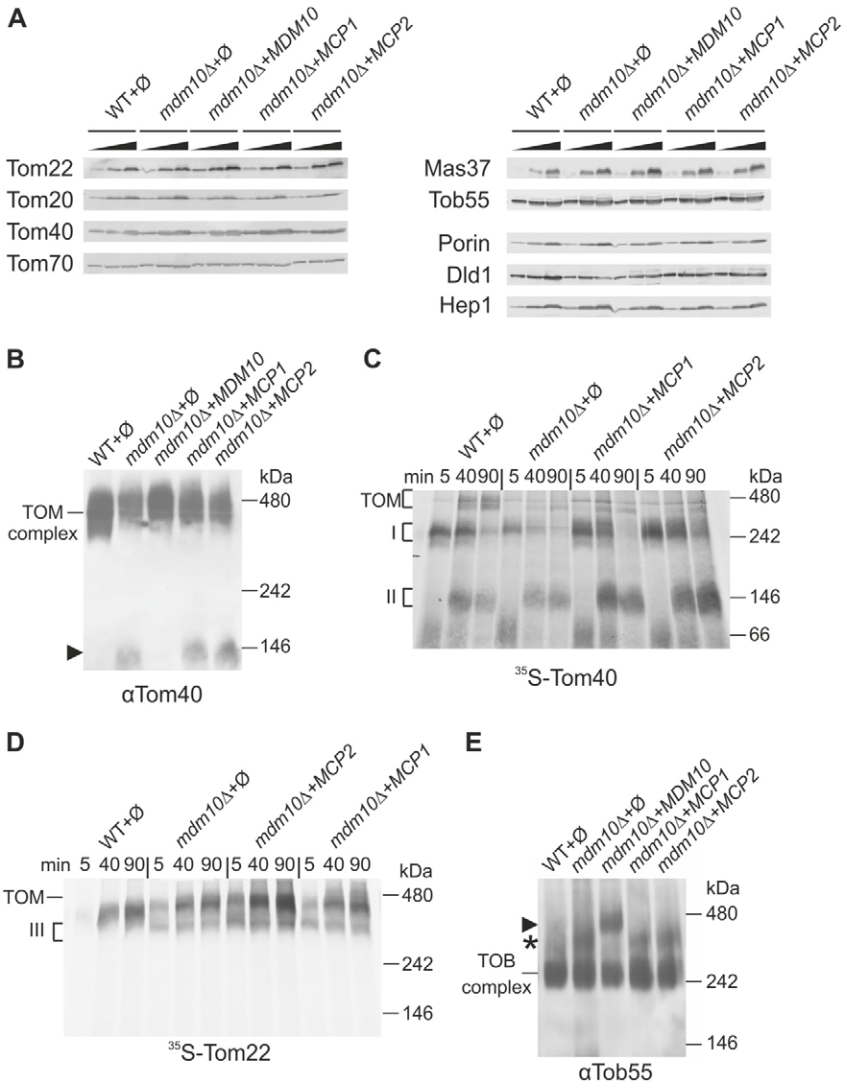


**Fig. 5. Overexpression of Mcp1 or Mcp2 in *mdm10*Δ cells does not influence steady state levels of mitochondrial proteins and TOM or TOB complex assembly.** (**A**) Increasing amounts (10, 30 and 60 µg) of mitochondria isolated from the specified strains were analysed by SDS-PAGE and immunodecorated with the indicated antibodies. A representative experiment of three independent repeats is presented. (**B**) Mitochondria of the indicated strains were lysed in 1% digitonin and subjected to BN-PAGE and immunoblotting with an antibody against Tom40. The assembled TOM complex and an unassembled Tom40 species at ca. 100 kDa (arrowhead) are indicated. (**C**) Radiolabeled precursor molecules of Tom40 were imported for various time periods into mitochondria isolated from the indicated strains. After import, the mitochondria were solubilized with digitonin and analysed by BN-PAGE and autoradiography. The two assembly intermediates (I and II) of Tom40 as well as the assembled TOM core complex (TOM) are indicated. (**D**) Radiolabeled precursor molecules of Tom22 were imported and mitochondria were treated as described in C. The assembly intermediate of Tom22 (III) (Meisinger et al., 2004) as well as the assembled TOM core complex (TOM) are indicated. (**E**) Mitochondria of the indicated strains were lysed in 0.5% Triton X-100 and subjected to BN-PAGE and immunoblotting with antibody against Tob55. The TOB core complex is indicated. Two additional higher molecular mass species of the TOB complex are marked by an arrowhead and an asterisk (they are discussed in the text).

It is well documented that alterations in Mdm10 levels affect the amounts of various forms of the TOB complex (Thornton et al., 2010; Yamano et al., 2010b; Yamano et al., 2010a; Becker et al., 2011). In agreement with these reports, we observed three different TOB-complex species (Fig. 5E). In wild-type cells we observed the TOB core complex (containing Tob55, Tob38 and Mas37) as the main form. Upon loss of Mdm10, a larger complex became visible (Fig. 5E, second lane, asterisk). This complex resembles the reported TOB–Tom5/Tom40 species (Thornton et al., 2010). Overexpression of Mdm10 led to an additional TOB complex form that migrates like the previously reported TOB–Mdm10 holo-complex (Meisinger et al., 2004; Yamano et al., 2010b). Since upon overexpression of Mcp1 and Mcp2 we still observed the same TOB complex pattern as for *mdm10*Δ cells, we propose that Mcp1 and Mcp2 are not involved in the biogenesis and/or assembly of the TOB complex.

### Mcp1 and Mcp2 suppress the growth phenotypes of cells lacking Mmm1, Mmm2 or Mdm12

We next asked whether Mcp1 or Mcp2 are functionally related to the other subunits of the ERMES complex. To study the genetic interaction of Mcp1 or Mcp2 with other ERMES components we overexpressed the Mdm10 supressors in *mmm1*Δ, *mmm2*Δ or *mdm12*Δ cells. Mcp1 and Mcp2 could rescue (completely or partially) the loss of each of the ERMES subunits (see representative clones in Fig. 6A–C). To substantiate these results, we tested at least three different clones of each rescue transformation and compared them to two transformants harbouring the empty plasmid (supplementary material Fig. S7 and data not shown). Interestingly Mcp2 is a better suppressor for loss of Mdm12 whereas Mcp1 is more efficient in suppressing the *mmm1*Δ and *mmm2*Δ phenotypes. These results show that Mcp1 and Mcp2 have distinct functions and both can compensate for the loss of functional ER–mitochondria tethering complex ERMES.

### Assembly of respiratory supercomplexes is restored upon overexpression of Mcp1 and Mcp2

The respiratory chain complexes form supercomplexes that can be assessed by BN-PAGE and Coomassie staining and/or immunodecoration (Schägger, 2001). We realized that the supercomplex pattern of mitochondria lacking Mdm10 is altered in comparison to wild-type organelles and this assembly phenotype can be reversed by overexpression of Mdm10 itself, Mcp1 or Mcp2 (Fig. 7A). To verify the identity of these

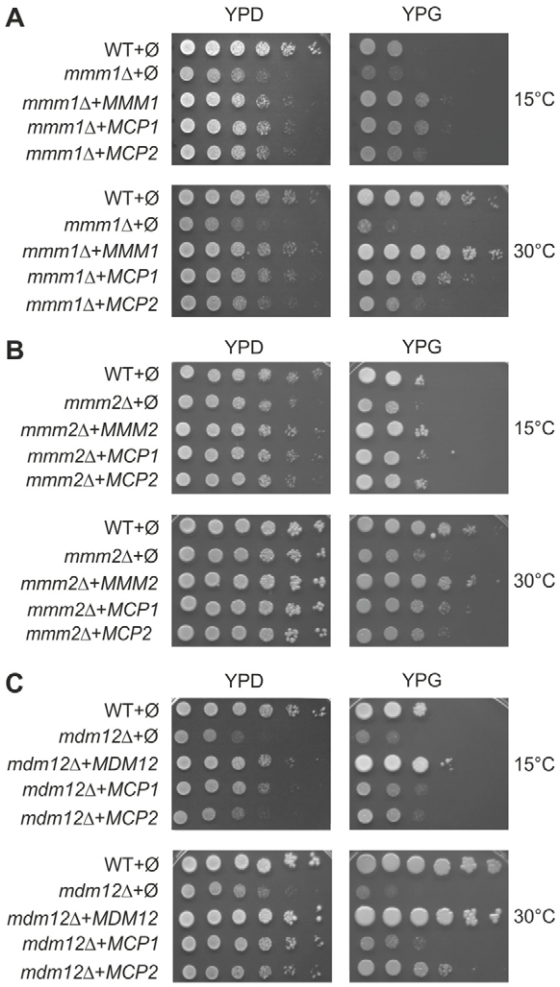


**Fig. 6. Overexpression of Mcp1 and Mcp2 can suppress the growth phenotype of *mmm1Δ*, *mmm2*Δ and *mdm12Δ* cells.** (**A**) Wild-type or *mmm1*Δ cells transformed with the empty plasmid pYX142 (Ø) or *mmm1*Δ cells overexpressing Mcp1, Mcp2 or Mmm1 (as a control) were analysed at 15℃ or 30℃ by drop dilution assay on rich medium containing either glucose (YPD) or glycerol (YPG). (**B**) Wild-type and *mmm2*Δ cells were transformed and analysed as described in A. (**C**) Wild-type and *mdm12*Δ cells were transformed and analysed as described in A.

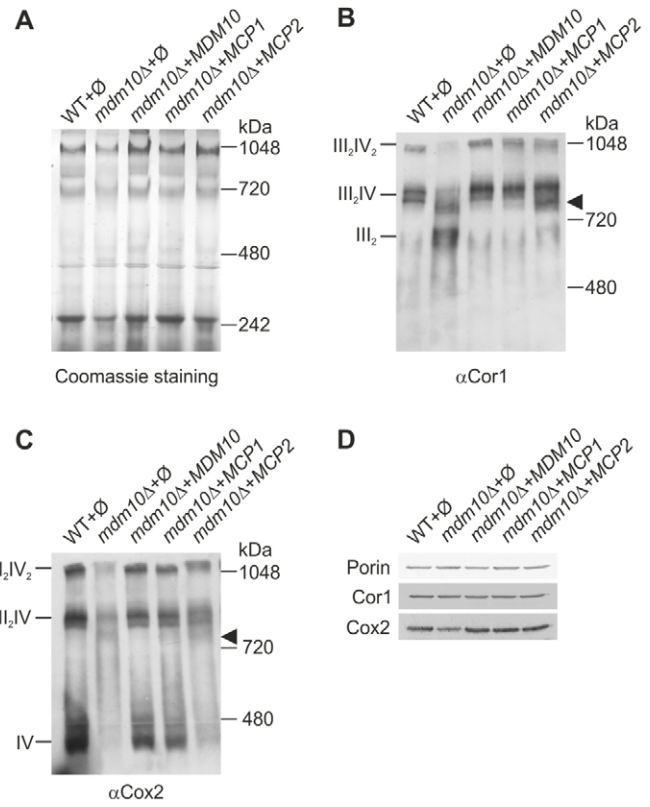


**Fig. 7. Overexpression of Mcp1 or Mcp2 in *mdm10*Δ cells rescues the assembly phenotype of respiratory chain supercomplexes.** (**A**) Mitochondria isolated from the indicated strains were lysed in 1% digitonin and subjected to a 4–8% BN-PAGE. The gel was stained with Coomassie Brilliant Blue G-250. (**B**,**C**) Mitochondria were analysed by BN-PAGE as described in A, proteins were blotted onto a PVDF membrane and analysed by immunodecoration with an antibody against either the subunit Cor1 of complex III (B) or the subunit Cox2 of complex IV (C). Supercomplexes of the respiratory chain complexes are indicated. (**D**) Mitochondria (20 μg) isolated from the indicated strains were lysed in 1% digitonin as for BN-PAGE and then solubilized proteins were subjected to SDS-PAGE and analysed with antibodies against Porin, Cor1 and Cox2.

supercomplexes we immunodecorated mitochondrial proteins separated by BN-PAGE with antibodies specific for subunits of complex III (Cor1) and complex IV (Cox2) of the oxidative phosphorylation (OXPHOS) pathway. Indeed, we observed a dramatic change of OXPHOS complex and supercomplex patterns in *mdm10*Δ cells (Fig. 7B,C). Upon immunodecoration with an antibody specific for Cor1, we observed an increase in the amount of the complex III dimer ($III_2$) and a strong decrease of the complex III/IV hetero-tetramer and trimer ($III_2IV_2$, $III_2IV$). In addition, we detected an additional band of around 750 kDa of unknown composition (Fig. 7B, arrowhead). Overexpression of Mcp1, similarly to the re-introduction of Mdm10 itself, lead to a complete rescue of the migration pattern (Fig. 7B). Overexpression of Mcp2 resulted in a partial complementation of the defect in the formation of III/IV supercomplexes. Although the upper band of the $III_2IV$ hetero-trimer and the tetramer $III_2IV_2$ were restored, the lower trimer band was missing and the additional band at 750 kD was still visible (Fig. 7B, last lane). Similar complementation capacities were observed upon immunodecoration with an antibody against the complex IV subunit Cox2. There is an additional band at 750 kDa that remains upon Mcp2 overexpression (Fig. 7C arrowhead). Yet the trimer and the tetramer are restored in case of the overexpression of Mcp1, Mcp2 and as a control Mdm10 (Fig. 7C). Of note the steady-state levels of the mitochondrially encoded Cox2 are slightly decreased in *mdm10*Δ cells (Fig. 7D). This is probably due to either the reported alterations in mitochondrial DNA and nucleoid phenotype in *mdm10*Δ cells (Sogo and Yaffe, 1994) or the reduced stability of the protein in the membrane. This reduction in the steady-state levels could be restored by overexpression of Mdm10 and its two suppressors (Fig. 7D). Taken together, overexpression of Mcp1 or Mcp2 rescued defects in respiratory chain protein complex assembly derived by the loss of Mdm10.

### Overexpression of Mcp1 and Mcp2 partially restores the lipid composition of *mdm10*Δ mitochondria

It was previously shown that the lipid composition of mitochondria and especially cardiolipin levels affect the

biogenesis and function of protein complexes in mitochondrial membranes (Jiang et al., 2000; Schägger, 2002; Zhang et al., 2002; Pfeiffer et al., 2003; Zhong et al., 2004; Nury et al., 2005; Zhang et al., 2005; van der Laan et al., 2007; Claypool et al., 2008; Kutik et al., 2008). Furthermore, there are several reports that loss of Mdm10 and defects in the ERMES complex result in an altered phospholipid composition of mitochondria (Kornmann et al., 2009; Osman et al., 2009; Yamano et al., 2010b; Nguyen et al., 2012; Tamura et al., 2012a). We wondered whether the rescue by Mcp1 and Mcp2 overexpression can be explained by changes in the lipid contents of mitochondria. To this end we analysed by mass spectrometry the lipid composition of mitochondria isolated from the strains of interest.

As reported before, the loss of Mdm10 led to a change in phospholipid composition of mitochondria. Especially phosphatidylethanolamine (PE) and cardiolipin (CL) levels were reduced, whereas the relative amounts of phosphatidylserine (PS) were increased (Fig. 8A; supplementary material Table S1) (Kornmann et al., 2009; Osman et al., 2009; Yamano et al., 2010b; Nguyen et al., 2012; Tamura et al., 2012a). We also analysed the different species of the single phospholipids upon deletion of *MDM10* and found an increase of the 34:2 species of PC, PE, PS and PI (supplementary material Table S2). Mcp1 overexpression could compensate for reduction of PE and increase in PS levels in *mdm10*Δ cells. Yet CL levels were only slightly restored. The effect of Mcp2 overexpression was less pronounced, still PE levels were back to wild-type values, CL levels were moderately increased and PS levels decreased in comparison to *mdm10*Δ cells (Fig. 8A; supplementary material Table S1). The fact that overexpression of Mcp1 leads to a better restoration of regular lipid composition is in agreement with the higher rescue capacity of this suppressor.

The deletion of *MCP1* or *MCP2* led only to minor changes in phospholipid composition of mitochondria. Most obvious is a minor statistically insignificant reduction of phosphatidylcholine (PC) in the case of *mcp1*Δ. Furthermore a very minor reduction in phosphatidylinositol (PI) amounts for *mcp2*Δ is visible (Fig. 8A; supplementary material Table S1).

Taken together, overexpression of Mcp1 and Mcp2 in *mdm10*Δ cells results in partial restoration of the altered phospholipid levels of these cells.

### Deletion of *MDM10* results in elevated ergosterol levels in mitochondria

Changes in mitochondrial phospholipid composition connected to the loss of ERMES function were reported before (Kornmann et al., 2009; Osman et al., 2009; Yamano et al., 2010b; Tamura et al., 2012a). Yet, an open question is whether Mdm10 is also involved in the regulation of ergosterol trafficking into and out of mitochondria. In this context we analysed the levels of ergosterol in mitochondria isolated from cells with altered levels of Mdm10, Mcp1 and Mcp2. The deletion of *MDM10* resulted in a twofold increase of the mitochondrial ergosterol levels. Of note, this increment was reversed by the overexpression of either Mdm10 itself or Mcp1 but not by overexpression of Mcp2. The deletion of each *MCP* did not alter the amounts of ergosterol (Fig. 8B;

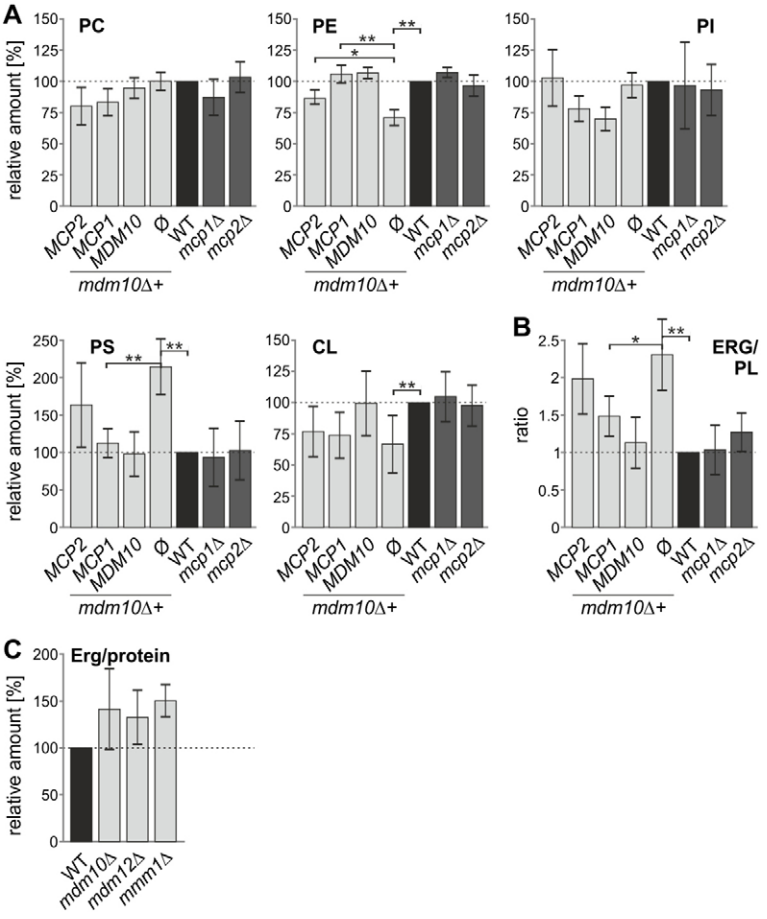


**Fig. 8. Overexpression of Mcp1 or Mcp2 partially restores the alterations in the lipid composition of mitochondria from *mdm10*Δ cells.** (**A**) Mitochondria were isolated from the indicated yeast cells and purified using percoll or a sucrose gradient. Lipids were extracted and then identified and quantified by mass spectrometry. The level of each phospholipid species in wild-type mitochondria was set to 100% and relative changes in mitochondria from other cells are presented. The means and standard deviations of three biological replicates, with two technical replicates for each ($n=6$) is given. $^{*}P<0.05$, $^{**}P<0.005$ (unpaired *t*-test, two-tailed). (**B**) Mitochondrial preparations as described in A were analysed for their ergosterol content and the values are presented as ERG/phospholipids (PL) molar ratio. For clarity, the wild-type control was set to 1.0 and the mean with standard deviation of three biological replicates with two technical replicates for each ($n=6$) are shown $^{*}P<0.05$, $^{**}P<0.005$ (unpaired *t*-test, two-tailed). (**C**) Mitochondrial preparations as described in A were analysed for ergosterol content and the results are presented as ERG/protein ratio. The wild-type control was set to 100% and the mean with standard deviation of three independent mitochondrial preparations are shown. PC, phosphatidylcholine; PE, phosphatidylethanolamine; PI, phosphatidylinositol; PS, phosphatidylserine; CL, cardiolipin; ERG, ergosterol.

supplementary material Table S1). We excluded the possibility that the restored ergosterol levels upon overexpression of Mcp1 are related to lower ER contamination in the purified mitochondria samples by immunodecoration of these samples with an antibody against the ER marker, Erv2 (supplementary material Fig. S8).

We next tested whether other ERMES components are also involved in ergosterol homeostasis. To this end we compared the ergosterol content of mitochondria isolated from *mdm10Δ*, *mdm12Δ* and *mmm1Δ* cells grown on rich medium to that in organelles from wild-type cells. As shown in Fig. 8C, loss of Mdm10, Mdm12 or Mmm1 leads to an ~50% increase of ergosterol in comparison to wild-type mitochondria. Hence, these results indicate an important novel role for Mdm10 and the ERMES complex in the homeostasis of ergosterol in mitochondria, and might suggest a role for Mcp1 in this process.

### Severe negative genetic interactions of *MCP1* and *MCP2* with ERMES components

The aforementioned functional links of the Mcp proteins to ERMES components lead us to investigate whether the deletion of *MCP1* or *MCP2* shows genetic interactions with deletions of the ERMES components. To this end we mated haploid W303 cells lacking Mcp1 or Mcp2 (*mcp1Δ* or *mcp2Δ*) with cells lacking one of the ERMES components (*mmm1Δ*, *mmm2Δ*, *mdm10Δ* or *mdm12Δ*) of the opposing mating type. After selection for the heterologous diploid double deletion strains W303a/α and sporulation we performed tetrad dissection. The summary of the results is shown in supplementary material Fig. S9A; *mcp1Δ* is synthetic lethal with *mdm10Δ*, *mmm2Δ* and the deletion of the ER protein encoding *MMM1*. Similarly, deletion of *MCP2* together with *MMM1* leads to inviable spores. supplementary material Fig. S9B illustrates the results of genetic lethal interactions. The arrowheads point to barely visible microcolonies identified by marker analysis of the other spores that did not grow further upon re-streaking on a novel plate. In those cases where the double deletion strains were viable (deletion of *MCP1* together with *MDM12* and *MCP2* with *MDM10*, *MDM12* or *MMM2*) we observed a severe negative synthetic growth defect most pronounced at higher temperatures (supplementary material Fig. S9C). Taken together, these results show a strong negative genetic interaction between either *MCP1* or *MCP2* with any of the ERMES components.

## Discussion

Mdm10 is a β-barrel protein that was shown to be involved in mitochondrial core functions like morphogenesis, inheritance, cytoskeleton interaction, biogenesis of β-barrel proteins, mitochondria–ER contact, and lipid transport. However, many of the aforementioned processes are inter-connected. For example, a decreased assembly of MOM import complexes can lead to reduced import of mitochondrial morphology proteins, which in turn would lead to a morphology phenotype. Along the same line, a compromised mitochondria–ER contact can result in hampered lipid flow between the involved compartments, changes of the lipid composition of their membranes and subsequently alteration in assembly of membrane-embedded complexes and/or in fusion of mitochondrial membranes. An altered mitochondrial lipid composition in the absence of Mdm10 is observed in many studies (Kornmann et al., 2009; Osman et al., 2009; Yamano et al., 2010b; Osman et al., 2011; Nguyen et al., 2012). Accordingly, Mdm10 was suggested to be involved in lipid homeostasis of mitochondria. Considering all these possibilities, the identification of the primary function of Mdm10 remains a central challenge.

In the present work we identified two novel mitochondrial proteins, which we named Mcp1 and Mcp2, as high-copy suppressors of the growth phenotype of *mdm10*Δ cells. Both proteins also suppress phenotypes that are related to altered lipid homeostasis in *mdm10*Δ cells but only marginally affect import defects in these cells. Thus, our findings suggest that the prominent function of Mdm10 is its contribution to lipid transport. Mcp1 and Mcp2 rescue OXPHOS supercomplex formation that is disturbed in *mdm10*Δ mitochondria and partially restore the lipid profile of the organelle. Supercomplex formation is restored almost completely, yet cardiolipin levels are only moderately rescued upon overexpression of Mcp1. On the other hand, PE quantities are even elevated in these mitochondria in comparison to organelles from wild-type cells. We propose that a certain threshold amount of non-bilayer forming lipids (PE and CL) is required for the proper formation of the OXPHOS supercomplexes. These two lipids can compensate for one another as also indicated by the observation that yeast cells cannot tolerate simultaneous reduction of CL and PE (Osman et al., 2011). Such a threshold is apparently not achieved in cells lacking Mdm10. The overexpression of Mcp1 and to a lower extent of Mcp2 restores the levels of CL and PE to a point above this critical amount, therefore restoring supercomplex formation. The recent identification of Mdm31 as another suppressor of the growth phenotype of *mdm10*Δ mutation supports this conclusion, as overexpression of Mdm31 in cells lacking Mdm10 restores the cardiolipin levels in these cells (Tamura et al., 2012a). In contrast, overexpression of components of the TOB or TOM complexes did not result in a rescue of the growth phenotype of *mdm10*Δ cells (data not shown). Of note, Mdm10 appears to have a unique role within the ERMES complex as our results indicate that overexpression of none of the other subunits of this complex could compensate for the absence of Mdm10.

How do Mcp1 and Mcp2 influence the lipid composition of mitochondria? Deletion of both genes has only minor influence on lipid levels. The importance of the two suppressors becomes obvious in the absence of a functional ERMES complex. Mcp1 and Mcp2 overexpression partially rescue the absence of each component of this ER–mitochondria connecting structure. Of note, despite various pull-down assays we were not able to obtain any evidence of a physical interaction of Mcp1 or Mcp2 with any of the ERMES complex subunits (data not shown). Supporting our findings are two recent studies set out to investigate the composition of the ERMES complex that have not identified other components of this complex besides Mdm10, Mdm12, Mmm1, Mmm2 and Gem1 (Kornmann et al., 2011; Stroud et al., 2011). Hence, we suggest that the MCP proteins are not associated with the ERMES complex but rather can provide an alternative pathway for lipid flow that ‘bypasses’ the requirement for the ERMES complex. The location of Mcp1 in the MOM positions it in an optimal place to facilitate such an exchange. A tempting yet speculative model would suggest an additional mitochondria–ER contact that functions as a back-up pathway for the known ERMES mediated inter-organellar lipid exchange. It is known that in higher eukaryotes apparently other mediators (like MFN2 and VDAC) contribute to ER–mitochondria association (for reviews, see de Brito and

Scorrano, 2010; Patergnani et al., 2011; Toulmay and Prinz, 2011). Indeed it was reported that although a defective ERMES complex impairs phospholipid exchange between ER and mitochondria it does not abolish it (Kornmann et al., 2009). Recent evidence even suggests that phosphatidylserine transport from the ER to mitochondria is not directly influenced by the ERMES complex (Nguyen et al., 2012), ruling out ERMES as the exclusive mediator of lipid exchange.

Further supporting such a scenario are the synthetic lethality or severe synthetic growth defects of double deletion strains of *mcp1Δ* and *mcp2Δ* in combination with a deletion of any of the four classical ERMES complex subunits. These genetic interactions substantiate the hypothesis that Mcp1 and Mcp2 are part of a 'bypass route' for lipids between the two compartments that can partially compensate for the major ERMES-facilitated pathway. The loss of both lipid exchange pathways would lead to a complete block of lipid exchange and thus to a lethal outcome. Such an alternative lipid transport pathway does not necessarily have to be between ER and mitochondria. For instance, it has been reported that a functional connection between mitochondria and the vacuole is mediated by the cardiolipin biosynthesis pathway (Chen et al., 2008), and a contact between mitochondria and lipid particles was also reported (Beller et al., 2010).

Because Mcp1 and Mcp2 play a role in lipid homeostasis of mitochondria, we wondered whether Mcp1 and Mcp2 are also suppressors of other genes known to be involved in lipid composition of the mitochondrial membranes. Ups1 and Ups2 are two proteins that were recently shown to be involved in the intra-mitochondrial lipid transport (Connerth et al., 2012; Tamura et al., 2012a). We overexpressed Mcp1 and Mcp2 in cells lacking Ups1 or Ups2 and did not observe any rescue effect (data not shown). These results support a role for the Mcps in global mitochondrial lipid transport rather than in intra-mitochondrial membrane lipid exchange.

Very recently, Mdm31 was identified as another high copy suppressor of *mdm10*Δ (Tamura et al., 2012a). Mdm31 was previously shown to be involved in mitochondrial morphogenesis, inheritance (Dimmer et al., 2005) and ion homeostasis (Kucejova et al., 2005). However, the precise molecular function of this protein is currently unknown. Although we screened about 30,000 colonies (about five times the number of genes of *S. cerevisiae*), Mdm31 was not amongst our candidates. Since it was previously reported that various phenotypes of ERMES mutants vary according to the genetic background (Yamano et al., 2010b), we suppose that our usage of another strain as compared with the one employed by Tamura et al. (Tamura et al., 2012a) can explain why Mdm31 was not identified in the present study.

Our findings provide for the first time evidence that, apart from the phospholipid composition of mitochondrial membranes, also ergosterol levels are affected by the ERMES complex. This observation has important implications for the potential influence of the ERMES complex on the biophysical properties of mitochondrial membranes. A higher ergosterol level, as observed in the *mdm10*Δ, *mmm1*Δ and *mdm*12Δ cells, results in more rigid membranes which would behave differently in respect to organelle morphology and membrane protein insertion. Similarly, it has been shown that downregulation of genes involved in ergosterol biosynthesis leads to a severe mitochondrial morphology phenotype (Altmann and Westermann, 2005), suggesting an important role of ergosterol in overall organelle morphogenesis. Furthermore, the proper membrane integration of some single-span mitochondrial MOM proteins requires a low ergosterol content of the membrane (Kemper et al., 2008; Krumpe et al., 2012; Merklinger et al., 2012). Moreover, it is tempting to assume that the function of protein translocases and especially insertases depends on the biophysical properties of the membrane they are embedded in and therefore on the lipid composition of these membranes. Indeed it has been shown, that the assembly of protein import complexes TOM, TIM22 and TIM23 depend on cardiolipin (Kutik et al., 2008; Gebert et al., 2009). Collectively, our observation that deletion of Mdm10 causes alteration in ergosterol content can help to explain part of the phenotypes of the *mdm10*Δ mutant.

Taken together, this study provides new insights into the regulation of the lipid composition of mitochondrial membranes. We show that Mdm10 plays a crucial role in ergosterol homeostasis of the organelle and two novel proteins Mcp1 and Mcp2 that are involved in mitochondrial lipid homeostasis were identified. These two proteins might be involved in an ERMES-independent pathway of lipid exchange to and from mitochondria.

## Materials and Methods

### Yeast strains and growth conditions

Yeast strains were grown in standard rich medium with either glucose (YPD) or glycerol (YPG), synthetic medium with either glucose (SD) or glycerol (SG), or lactate medium. For drop dilution assays, cells were cultured to an $OD_{600}$ of 1.0 and diluted in fivefold increment followed by spotting 5 µl of each cell suspension on the corresponding solid medium.

Standard genetic techniques were applied for the growth and manipulation of *Saccharomyces cerevisiae* cells. The strains used were isogenic to W303a and W303α. To delete complete open reading frames by homologous recombination the HIS3MX6 cassette was amplified from the plasmid pFA6a-HIS3MX6 (Wach et al., 1997) and the KanMX4 cassette from pFA6a-KanMX4 (Wach et al., 1994) with gene-specific primers. Primer sequences are listed in supplementary material Table S3. Double-deletion strains were obtained by tetrad dissection. All deletion strains were confirmed by genome based PCR with gene specific primers. Transformation of yeast strains was performed by the lithium acetate method.

### Recombinant DNA techniques

The open reading frames of *MDM10*, *MMM1*, *MMM2*, *MDM12*, *MCP1* and *MCP2* genes were amplified by PCR from yeast genomic DNA and cloned into the plasmid pYX142 that encodes an additional HA tag sequence. By omission of the stop codon of the ORFs, a plasmid-borne HA tag was introduced C-terminally to the coding sequence. All constructs were analysed by sequencing. Primer sequences are listed in supplementary material Table S3.

### Selection of the high-copy-number suppressors

Cells lacking Mdm10 (*mdm10*Δ) were transformed with a high-copy-number yeast genomic library constructed by F. Lacroute in the *URA3* 2 µ plasmid pFL44L (Stettler et al., 1993). Clones were initially selected at 30℃ on synthetic medium lacking uracil. Then clones were replica plated on glycerol-containing full medium and further selected at 37℃. Plasmid DNA was extracted from the clones grown at 37℃ and transformed into *E. coli* cells. The DNA inserts of plasmids isolated from the transformed *E. coli* cells were analysed by sequencing.

### Biochemical methods

Subcellular fractionation was performed according to published procedures (Walther et al., 2009). Mitochondria of yeast cells were isolated by differential centrifugation as described previously (Daum et al., 1982). Further purification of mitochondria was achieved via a self-generated percoll or sucrose step gradients (Graham, 2001). For swelling experiments, mitochondria were incubated in hypotonic buffer (20 mM Hepes, pH 7.2) for 30 minutes on ice. Proteins were retrieved by trichloroacetic acid (TCA) precipitation and solubilized in sample buffer. Mitochondrial MOM and MIM vesicles were generated and separated as described (Tamura et al., 2012b). After resuspension of the vesicles, sucrose concentration was adjusted to 0.85 M. A sucrose step gradient (0.9/1.0/1.1/1.2/1.3 M) was applied for separation and centrifugation was performed for 16 hours (200,000 ***g***, 4℃) in a Beckman SW60 rotor. Protein samples were analysed by SDS-PAGE and immunoblotting using the ECL system.

### Blue native PAGE

Mitochondria were lysed in 40 µl buffer containing either Triton X-100 or digitonin [0.5% Triton X-100 or 1–1.5% digitonin, 20 mM Tris-HCl, 0.1 mM EDTA, 50 mM NaCl, 10% (v/v) glycerol, 1 mM PMSF, pH 7.2]. After incubation

on ice for 15 min and clarifying spin (30,000 ***g***, 15 minutes, 2℃), 5 µl sample buffer [5% (w/v) Coomassie blue G, 500 mM 6-amino-*N*-caproic acid, 100 mM Bis-Tris, pH 7.0] was added, and the mixture was analysed by electrophoresis in a 6–13% or 4–8% gradient blue native gel (Schägger, 2002). Gels were blotted on polyvinylidene fluoride membranes and proteins were further analysed by autoradiography or immunodecoration.

#### *In vitro* import

Import experiments were carried out with radiolabeled precursor proteins and isolated mitochondria in import buffer (250 mM sucrose, 0.25 mg/ml BSA, 80 mM KCl, 5 mM $MgCl_2$, 10 mM MOPS-KOH, 2 mM NADH, and 2 mM ATP, pH 7.2). Radiolabeled precursor proteins were synthesized in the presence of [$^{35}$S]methionine in rabbit reticulocyte lysate (Promega, Mannheim, Germany) according to the manufacturer's protocol. Import reactions were performed for various time periods at 25℃. At the end of the import reaction, mitochondria were re-isolated by centrifugation (13,200 ***g***, 10 minutes, 2℃) and then analysed by SDS- or BN-PAGE.

#### Fluorescence microscopy

For visualization of mitochondria, yeast cells were transformed with an expression vector harbouring the mitochondrial presequence of subunit 9 of Fo-ATPase of *Neurospora crassa* fused to GFP or RFP (Mozdy et al., 2000; Westermann and Neupert, 2000). Microscopy images were acquired with an Axioskop20 fluorescence microscope equipped with an Axiocam MRm camera using the 43 Cy3 and 38 Endow GFP filter sets and the AxioVision software (Zeiss, Göttingen, Germany). For statistical analysis, yeast mitochondria were also visualized by staining with the mitochondria-specific dye rhodamine B hexyl ester (Life Technologies GmbH, Darmstadt, Germany).

#### Lipid component analysis

Cells at the log phase ($OD_{600}$<2.0) grown on selective medium containing galactose were harvested and mitochondria were isolated first by differential centrifugation and then crude organelles were purified further by a self-generated percoll gradient or sucrose step gradient (see above). Mass spectrometry analysis was performed in positive ion mode on a triple quadrupole-linear ion trap hybrid mass spectrometer (QTRAP 5500, AB Siex), except for analysis of cardiolipin and ergosterol, which was done in negative ion mode on a quadrupole time-of-flight mass spectrometer (QStar Elite, AB Siex). Lipid extractions (total lipid amount of 1.5–2.5 nmol) were performed in the presence of internal lipid standards [PC, PE, PS with species 14:1/14:20:1/20:1 and 22:1/22:1), PI (37:4), CL 56:0] (Lorizate et al., 2013). Dried lipids were dissolved in 10 mM ammonium acetate.

Quantification of PC was performed by precursor ion scanning, selecting for a fragment ion of 184 Da. PE, PS and PI were quantified by neutral loss scanning, selecting for a neutral loss of 141, 185 and 277 Da, respectively. For CL quantification, 10 µl of lipid extracts was diluted 1:2 with 0.1% piperidine in methanol and automatically infused (Triversa Nanomate, Advion Biosciences) (Osman et al., 2009). CLs were detected as single charged molecules. CL species were analysed by targeted product ion scanning. The peak areas of CL-derived fatty acid fragments were extracted from the respective product ion spectra via the 'Extract Fragments' script (Analyst QS 2.0). Isotope correction for M+2 ions was done manually. Ergosterol quantification was performed as described (Ejsing et al., 2009). Lipid species identification and data evaluation were performed with the LipidView software (ABSciex).

## Acknowledgements

We thank K. Rehn and E. Kracker for technical support, N. Bonnefoy for the yeast genomic library, D. Papić and F. Essmann for critically reading the manuscript as well as C. Ernst and A. Peschel for help with the lipid analysis. B.B. is an investigator of the Cell Networks Cluster of Excellence (EXC81).

## Author contributions

T.T., B.B., D.R. and K.S.D. designed research; T.T., C.O., and K.S.D. performed research; T.T., C.O., B.B., D.R. and K.S.D. analyzed data; and D.R. and K.S.D. wrote the paper.

## Funding

This work was supported by the Deutsche Forschungsgemeinschaft [grant numbers DR1028-4/1 to D.R., SFB/TRR83 to B.B.); and a postdoctoral fellowship from the Carl Zeiss Stiftung [grant number 21-0563-2.8/122/1 to K.S.D.].

Supplementary material available online at
http://jcs.biologists.org/lookup/suppl/doi:10.1242/jcs.121244/-/DC1

## References

**Altmann, K. and Westermann, B.** (2005). Role of essential genes in mitochondrial morphogenesis in Saccharomyces cerevisiae. *Mol. Biol. Cell* **16**, 5410-5417.

**Becker, T., Wenz, L. S., Thornton, N., Stroud, D., Meisinger, C., Wiedemann, N. and Pfanner, N.** (2011). Biogenesis of mitochondria: dual role of Tom7 in modulating assembly of the preprotein translocase of the outer membrane. *J. Mol. Biol.* **405**, 113-124.

**Beller, M., Thiel, K., Thul, P. J. and Jäckle, H.** (2010). Lipid droplets: a dynamic organelle moves into focus. *FEBS Lett.* **584**, 2176-2182.

**Berger, K. H., Sogo, L. F. and Yaffe, M. P.** (1997). Mdm12p, a component required for mitochondrial inheritance that is conserved between budding and fission yeast. *J. Cell Biol.* **136**, 545-553.

**Biegert, A., Mayer, C., Remmert, M., Söding, J. and Lupas, A. N.** (2006). The MPI Bioinformatics Toolkit for protein sequence analysis. *Nucleic Acids Res.* **34**, W335-W339.

**Boldogh, I., Vojtov, N., Karmon, S. and Pon, L. A.** (1998). Interaction between mitochondria and the actin cytoskeleton in budding yeast requires two integral mitochondrial outer membrane proteins, Mmm1p and Mdm10p. *J. Cell Biol.* **141**, 1371-1381.

**Boldogh, I. R., Nowakowski, D. W., Yang, H. C., Chung, H., Karmon, S., Royes, P. and Pon, L. A.** (2003). A protein complex containing Mdm10p, Mdm12p, and Mmm1p links mitochondrial membranes and DNA to the cytoskeleton-based segregation machinery. *Mol. Biol. Cell* **14**, 4618-4627.

**Burgess, S. M., Delannoy, M. and Jensen, R. E.** (1994). MMM1 encodes a mitochondrial outer membrane protein essential for establishing and maintaining the structure of yeast mitochondria. *J. Cell Biol.* **126**, 1375-1391.

**Chen, S., Tarsio, M., Kane, P. M. and Greenberg, M. L.** (2008). Cardiolipin mediates cross-talk between mitochondria and the vacuole. *Mol. Biol. Cell* **19**, 5047-5058.

**Claypool, S. M., Oktay, Y., Boontheung, P., Loo, J. A. and Koehler, C. M.** (2008). Cardiolipin defines the interactome of the major ADP/ATP carrier protein of the mitochondrial inner membrane. *J. Cell Biol.* **182**, 937-950.

**Connerth, M., Tatsuta, T., Haag, M., Klecker, T., Westermann, B. and Langer, T.** (2012). Intramitochondrial transport of phosphatidic acid in yeast by a lipid transfer protein. *Science* **338**, 815-818.

**Dallabona, C., Marsano, R. M., Arzuffi, P., Ghezzi, D., Mancini, P., Zeviani, M., Ferrero, I. and Donnini, C.** (2010). Sym1, the yeast ortholog of the MPV17 human disease protein, is a stress-induced bioenergetic and morphogenetic mitochondrial modulator. *Hum. Mol. Genet.* **19**, 1098-1107.

**Daum, G. and Vance, J. E.** (1997). Import of lipids into mitochondria. *Prog. Lipid Res.* **36**, 103-130.

**Daum, G., Gasser, S. M. and Schatz, G.** (1982). Import of proteins into mitochondria. Energy-dependent, two-step processing of the intermembrane space enzyme cytochrome b2 by isolated yeast mitochondria. *J. Biol. Chem.* **257**, 13075-13080.

**de Brito, O. M. and Scorrano, L.** (2010). An intimate liaison: spatial organization of the endoplasmic reticulum-mitochondria relationship. *EMBO J.* **29**, 2715-2723.

**Dimmer, K. S., Fritz, S., Fuchs, F., Messerschmitt, M., Weinbach, N., Neupert, W. and Westermann, B.** (2002). Genetic basis of mitochondrial function and morphology in Saccharomyces cerevisiae. *Mol. Biol. Cell* **13**, 847-853.

**Dimmer, K. S., Jakobs, S., Vogel, F., Altmann, K. and Westermann, B.** (2005). Mdm31 and Mdm32 are inner membrane proteins required for maintenance of mitochondrial shape and stability of mitochondrial DNA nucleoids in yeast. *J. Cell Biol.* **168**, 103-115.

**Ejsing, C. S., Sampaio, J. L., Surendranath, V., Duchoslav, E., Ekroos, K., Klemm, R. W., Simons, K. and Shevchenko, A.** (2009). Global analysis of the yeast lipidome by quantitative shotgun mass spectrometry. *Proc. Natl. Acad. Sci. USA* **106**, 2136-2141.

**Gebert, N., Joshi, A. S., Kutik, S., Becker, T., McKenzie, M., Guan, X. L., Mooga, V. P., Stroud, D. A., Kulkarni, G., Wenk, M. R. et al.** (2009). Mitochondrial cardiolipin involved in outer-membrane protein biogenesis: implications for Barth syndrome. *Curr. Biol.* **19**, 2133-2139.

**Graham, J. M.** (2001). Purification of a crude mitochondrial fraction by density-gradient centrifugation. *Curr. Protoc Cell Biol.* **4**, 3.4.1-3.4.22.

**Hahne, K., Haucke, V., Ramage, L. and Schatz, G.** (1994). Incomplete arrest in the outer membrane sorts NADH-cytochrome b5 reductase to two different submitochondrial compartments. *Cell* **79**, 829-839.

**Huh, W. K., Falvo, J. V., Gerke, L. C., Carroll, A. S., Howson, R. W., Weissman, J. S. and O'Shea, E. K.** (2003). Global analysis of protein localization in budding yeast. *Nature* **425**, 686-691.

**Jiang, F., Ryan, M. T., Schlame, M., Zhao, M., Gu, Z., Klingenberg, M., Pfanner, N. and Greenberg, M. L.** (2000). Absence of cardiolipin in the crd1 null mutant results in decreased mitochondrial membrane potential and reduced mitochondrial function. *J. Biol. Chem.* **275**, 22387-22394.

**Kemper, C., Habib, S. J., Engl, G., Heckmeyer, P., Dimmer, K. S. and Rapaport, D.** (2008). Integration of tail-anchored proteins into the mitochondrial outer membrane does not require any known import components. *J. Cell Sci.* **121**, 1990-1998.

**Kornmann, B., Currie, E., Collins, S. R., Schuldiner, M., Nunnari, J., Weissman, J. S. and Walter, P.** (2009). An ER-mitochondria tethering complex revealed by a synthetic biology screen. *Science* **325**, 477-481.

**Kornmann, B., Osman, C. and Walter, P.** (2011). The conserved GTPase Gem1 regulates endoplasmic reticulum-mitochondria connections. *Proc. Natl. Acad. Sci. USA* **108**, 14151-14156.

**Krumpe, K., Frumkin, I., Herzig, Y., Rimon, N., Özbalci, C., Brügger, B., Rapaport, D. and Schuldiner, M.** (2012). Ergosterol content specifies targeting of tail-anchored proteins to mitochondrial outer membranes. *Mol. Biol. Cell* **23**, 3927-3935.

**Kucejova, B., Kucej, M., Petrezselyova, S., Abelovska, L. and Tomaska, L.** (2005). A screen for nigericin-resistant yeast mutants revealed genes controlling mitochondrial volume and mitochondrial cation homeostasis. *Genetics* **171**, 517-526.

**Kutik, S., Rissler, M., Guan, X. L., Guiard, B., Shui, G., Gebert, N., Heacock, P. N., Rehling, P., Dowhan, W., Wenk, M. R. et al.** (2008). The translocator maintenance protein Tam41 is required for mitochondrial cardiolipin biosynthesis. *J. Cell Biol.* **183**, 1213-1221.

**Lorizate, M., Sachsenheimer, T., Glass, B., Habermann, A., Gerl, M. J., Kräusslich, H. G. and Brügger, B.** (2013). Comparative lipidomics analysis of HIV-1 particles and their producer cell membrane in different cell lines. *Cell. Microbiol.* **15**, 292-304.

**Meisinger, C., Rissler, M., Chacinska, A., Szklarz, L. K., Milenkovic, D., Kozjak, V., Schönfisch, B., Lohaus, C., Meyer, H. E., Yaffe, M. P. et al.** (2004). The mitochondrial morphology protein Mdm10 functions in assembly of the preprotein translocase of the outer membrane. *Dev. Cell* **7**, 61-71.

**Merklinger, E., Gofman, Y., Kedrov, A., Driessen, A. J., Ben-Tal, N., Shai, Y. and Rapaport, D.** (2012). Membrane integration of a mitochondrial signal-anchored protein does not require additional proteinaceous factors. *Biochem. J.* **442**, 381-389.

**Model, K., Meisinger, C., Prinz, T., Wiedemann, N., Truscott, K. N., Pfanner, N. and Ryan, M. T.** (2001). Multistep assembly of the protein import channel of the mitochondrial outer membrane. *Nat. Struct. Biol.* **8**, 361-370.

**Mozdy, A. D., McCaffery, J. M. and Shaw, J. M.** (2000). Dnm1p GTPase-mediated mitochondrial fission is a multi-step process requiring the novel integral membrane component Fis1p. *J. Cell Biol.* **151**, 367-380.

**Nguyen, T. T., Lewandowska, A., Choi, J. Y., Markgraf, D. F., Junker, M., Bilgin, M., Ejsing, C. S., Voelker, D. R., Rapoport, T. A. and Shaw, J. M.** (2012). Gem1 and ERMES do not directly affect phosphatidylserine transport from ER to mitochondria or mitochondrial inheritance. *Traffic* **13**, 880-890.

**Nury, H., Dahout-Gonzalez, C., Trézéguet, V., Lauquin, G., Brandolin, G. and Pebay-Peyroula, E.** (2005). Structural basis for lipid-mediated interactions between mitochondrial ADP/ATP carrier monomers. *FEBS Lett.* **579**, 6031-6036.

**Okamoto, K. and Shaw, J. M.** (2005). Mitochondrial morphology and dynamics in yeast and multicellular eukaryotes. *Annu. Rev. Genet.* **39**, 503-536.

**Osman, C., Haag, M., Potting, C., Rodenfels, J., Dip, P. V., Wieland, F. T., Brügger, B., Westermann, B. and Langer, T.** (2009). The genetic interactome of prohibitins: coordinated control of cardiolipin and phosphatidylethanolamine by conserved regulators in mitochondria. *J. Cell Biol.* **184**, 583-596.

**Osman, C., Voelker, D. R. and Langer, T.** (2011). Making heads or tails of phospholipids in mitochondria. *J. Cell Biol.* **192**, 7-16.

**Paschen, S. A., Waizenegger, T., Stan, T., Preuss, M., Cyrklaff, M., Hell, K., Rapaport, D. and Neupert, W.** (2003). Evolutionary conservation of biogenesis of beta-barrel membrane proteins. *Nature* **426**, 862-866.

**Patergnani, S., Suski, J. M., Agnoletto, C., Bononi, A., Bonora, M., De Marchi, E., Giorgi, C., Marchi, S., Missiroli, S., Poletti, F. et al.** (2011). Calcium signaling around Mitochondria Associated Membranes (MAMs). *Cell Commun. Signal.* **9**, 19.

**Pfeiffer, K., Gohil, V., Stuart, R. A., Hunte, C., Brandt, U., Greenberg, M. L. and Schägger, H.** (2003). Cardiolipin stabilizes respiratory chain supercomplexes. *J. Biol. Chem.* **278**, 52873-52880.

**Reinders, J., Zahedi, R. P., Pfanner, N., Meisinger, C. and Sickmann, A.** (2006). Toward the complete yeast mitochondrial proteome: multidimensional separation techniques for mitochondrial proteomics. *J. Proteome Res.* **5**, 1543-1554.

**Reinhold, R., Krüger, V., Meinecke, M., Schulz, C., Schmidt, B., Grunau, S. D., Guiard, B., Wiedemann, N., van der Laan, M., Wagner, R. et al.** (2012). The channel-forming Sym1 protein is transported by the TIM23 complex in a presequence-independent manner. *Mol. Cell. Biol.* **32**, 5009-5021.

**Rowland, A. A. and Voeltz, G. K.** (2012). Endoplasmic reticulum-mitochondria contacts: function of the junction. *Nat. Rev. Mol. Cell Biol.* **13**, 607-625.

**Schägger, H.** (2001). Respiratory chain supercomplexes. *IUBMB Life* **52**, 119-128.

**Schägger, H.** (2002). Respiratory chain supercomplexes of mitochondria and bacteria. *Biochim. Biophys. Acta* **1555**, 154-159.

**Sogo, L. F. and Yaffe, M. P.** (1994). Regulation of mitochondrial morphology and inheritance by Mdm10p, a protein of the mitochondrial outer membrane. *J. Cell Biol.* **126**, 1361-1373.

**Stettler, S., Chiannilkulchai, N., Hermann-Le Denmat, S., Lalo, D., Lacroute, F., Sentenac, A. and Thuriaux, P.** (1993). A general suppressor of RNA polymerase I, II and III mutations in Saccharomyces cerevisiae. *Mol. Gen. Genet.* **239**, 169-176.

**Stroud, D. A., Oeljeklaus, S., Wiese, S., Bohnert, M., Lewandrowski, U., Sickmann, A., Guiard, B., van der Laan, M., Warscheid, B. and Wiedemann, N.** (2011). Composition and topology of the endoplasmic reticulum-mitochondria encounter structure. *J. Mol. Biol.* **413**, 743-750.

**Tamura, Y., Onguka, O., Hobbs, A. E., Jensen, R. E., Iijima, M., Claypool, S. M. and Sesaki, H.** (2012a). Role for two conserved intermembrane space proteins, Ups1p and Ups2p, [corrected] in intra-mitochondrial phospholipid trafficking. *J. Biol. Chem.* **287**, 15205-15218.

**Tamura, Y., Onguka, O., Itoh, K., Endo, T., Iijima, M., Claypool, S. M. and Sesaki, H.** (2012b). Phosphatidylethanolamine biosynthesis in mitochondria: phosphatidylserine (PS) trafficking is independent of a PS decarboxylase and intermembrane space proteins UPS1P and UPS2P. *J. Biol. Chem.* **287**, 43961-43971.

**Thornton, N., Stroud, D. A., Milenkovic, D., Guiard, B., Pfanner, N. and Becker, T.** (2010). Two modular forms of the mitochondrial sorting and assembly machinery are involved in biogenesis of α-helical outer membrane proteins. *J. Mol. Biol.* **396**, 540-549.

**Toulmay, A. and Prinz, W. A.** (2011). Lipid transfer and signaling at organelle contact sites: the tip of the iceberg. *Curr. Opin. Cell Biol.* **23**, 458-463.

**Trott, A. and Morano, K. A.** (2004). SYM1 is the stress-induced Saccharomyces cerevisiae ortholog of the mammalian kidney disease gene Mpv17 and is required for ethanol metabolism and tolerance during heat shock. *Eukaryot. Cell* **3**, 620-631.

**van der Laan, M., Meinecke, M., Dudek, J., Hutu, D. P., Lind, M., Perschil, I., Guiard, B., Wagner, R., Pfanner, N. and Rehling, P.** (2007). Motor-free mitochondrial presequence translocase drives membrane integration of preproteins. *Nat. Cell Biol.* **9**, 1152-1159.

**Wach, A., Brachat, A., Pöhlmann, R. and Philippsen, P.** (1994). New heterologous modules for classical or PCR-based gene disruptions in Saccharomyces cerevisiae. *Yeast* **10**, 1793-1808.

**Wach, A., Brachat, A., Alberti-Segui, C., Rebischung, C. and Philippsen, P.** (1997). Heterologous HIS3 marker and GFP reporter modules for PCR-targeting in Saccharomyces cerevisiae. *Yeast* **13**, 1065-1075.

**Walther, D. M., Papic, D., Bos, M. P., Tommassen, J. and Rapaport, D.** (2009). Signals in bacterial beta-barrel proteins are functional in eukaryotic cells for targeting to and assembly in mitochondria. *Proc. Natl. Acad. Sci. USA* **106**, 2531-2536.

**Westermann, B. and Neupert, W.** (2000). Mitochondria-targeted green fluorescent proteins: convenient tools for the study of organelle biogenesis in Saccharomyces cerevisiae. *Yeast* **16**, 1421-1427.

**Wideman, J. G., Go, N. E., Klein, A., Redmond, E., Lackey, S. W., Tao, T., Kalbacher, H., Rapaport, D., Neupert, W. and Nargang, F. E.** (2010). Roles of the Mdm10, Tom7, Mdm12, and Mmm1 proteins in the assembly of mitochondrial outer membrane proteins in Neurospora crassa. *Mol. Biol. Cell* **21**, 1725-1736.

**Wiedemann, N., Kozjak, V., Chacinska, A., Schönfisch, B., Rospert, S., Ryan, M. T., Pfanner, N. and Meisinger, C.** (2003). Machinery for protein sorting and assembly in the mitochondrial outer membrane. *Nature* **424**, 565-571.

**Yamano, K., Tanaka-Yamano, S. and Endo, T.** (2010a). Tom7 regulates Mdm10-mediated assembly of the mitochondrial import channel protein Tom40. *J. Biol. Chem.* **285**, 41222-41231.

**Yamano, K., Tanaka-Yamano, S. and Endo, T.** (2010b). Mdm10 as a dynamic constituent of the TOB/SAM complex directs coordinated assembly of Tom40. *EMBO Rep.* **11**, 187-193.

**Youngman, M. J., Hobbs, A. E., Burgess, S. M., Srinivasan, M. and Jensen, R. E.** (2004). Mmm2p, a mitochondrial outer membrane protein required for yeast mitochondrial shape and maintenance of mtDNA nucleoids. *J. Cell Biol.* **164**, 677-688.

**Zahedi, R. P., Sickmann, A., Boehm, A. M., Winkler, C., Zufall, N., Schönfisch, B., Guiard, B., Pfanner, N. and Meisinger, C.** (2006). Proteomic analysis of the yeast mitochondrial outer membrane reveals accumulation of a subclass of preproteins. *Mol. Biol. Cell* **17**, 1436-1450.

**Zhang, M., Mileykovskaya, E. and Dowhan, W.** (2002). Gluing the respiratory chain together. Cardiolipin is required for supercomplex formation in the inner mitochondrial membrane. *J. Biol. Chem.* **277**, 43553-43556.

**Zhang, M., Mileykovskaya, E. and Dowhan, W.** (2005). Cardiolipin is essential for organization of complexes III and IV into a supercomplex in intact yeast mitochondria. *J. Biol. Chem.* **280**, 29403-29408.

**Zhong, Q., Gohil, V. M., Ma, L. and Greenberg, M. L.** (2004). Absence of cardiolipin results in temperature sensitivity, respiratory defects, and mitochondrial DNA instability independent of pet56. *J. Biol. Chem.* **279**, 32294-32300.

Mcp1 and Mcp2, two novel proteins involved in mitochondrial lipid homeostasis

Supplementary Material

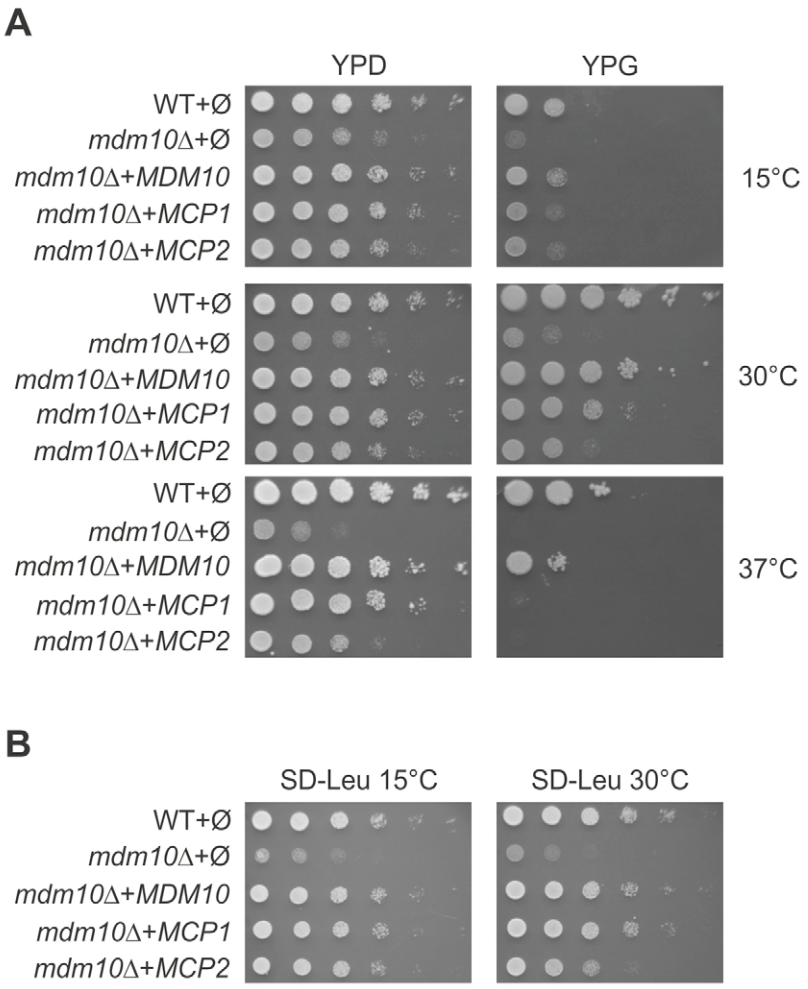


**Figure S1. Mcp1 and Mcp2 are multi-copy suppressors of *mdm10*Δ.** **(A)** Overnight cultures of the indicated strains were diluted in glucose-containing rich medium and grown to logarithmic phase. Serial 5-fold dilutions were spotted onto plates containing glucose (YPD) or glycerol (YPG) rich medium and cells were incubated at the indicated temperatures. **(B)** The indicated cells were grown on synthetic medium containing glucose and lacking leucine (SD-Leu). Serial 5-fold dilutions were spotted onto SD-Leu and incubated at 15°C or 30°C.

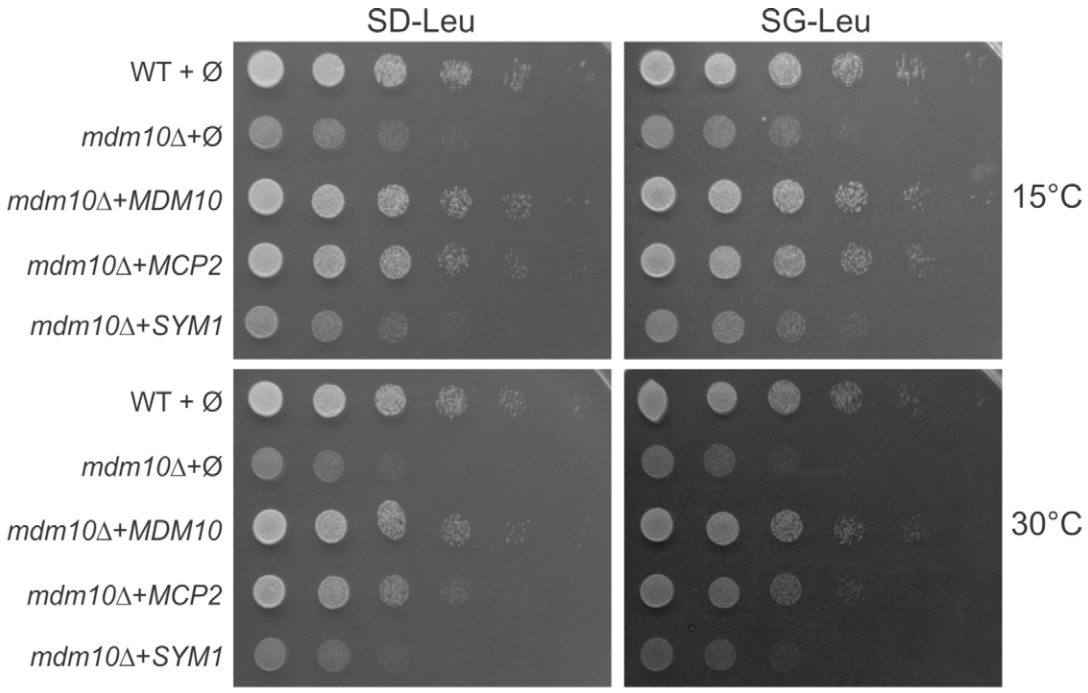


**Figure S2. Sym1 is not a multi-copy suppressor of *mdm10*Δ.** Overnight cultures of the indicated strains were diluted in glucose or glycerol containing selective medium (SD-Leu or SG-Leu respectively) and grown to logarithmic phase. Serial 5-fold dilutions were spotted onto plates containing the indicated medium and cells were incubated at the specified temperatures.

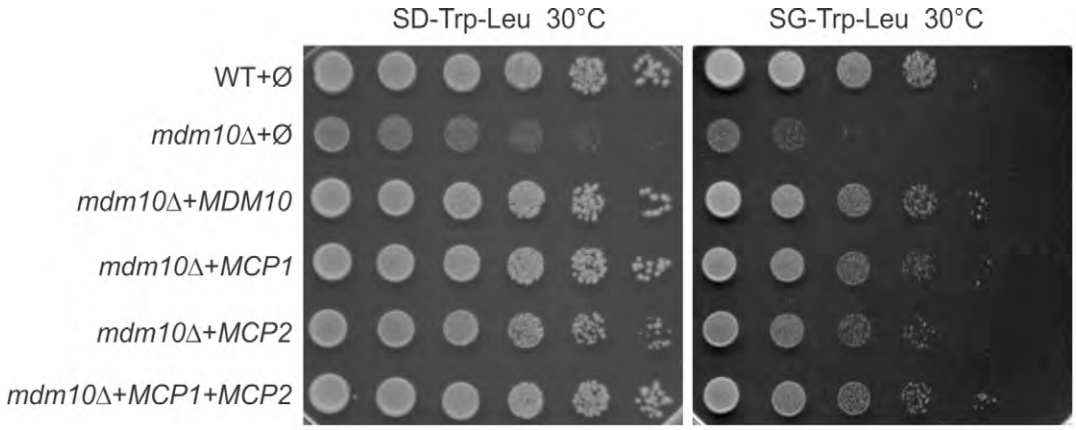


**Figure S3. Simultaneously over-expression of both Mcp1 and Mcp2 has no synergistic rescue effect on *mdm10*Δ growth phenotype.** Overnight cultures of the indicated strains were diluted in selective glucose or glycerol containing medium (SD-Trp-Leu or SG-Trp-Leu, respectively) and grown to logarithmic phase. Serial 5-fold dilutions were spotted onto plates with the indicated medium and incubated at 30°C.

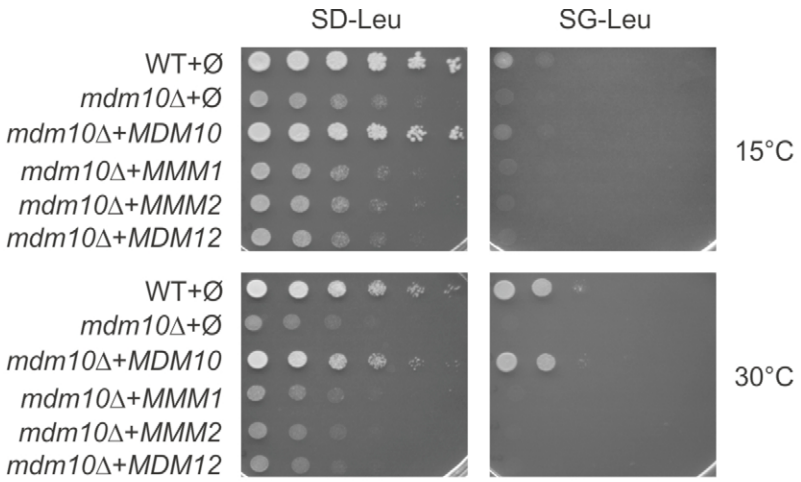


**Figure S4. Over-expression of other ERMES subunits does not rescue the *mdm10*Δ growth phenotype.** Overnight cultures of the indicated strains were diluted in selective glucose-containing medium and grown to logarithmic phase. Serial 5-fold dilutions were spotted onto plates with selective medium containing either glucose (SD-Leu) or glycerol (SG-Leu) and incubated at either 30°C or 15°C.

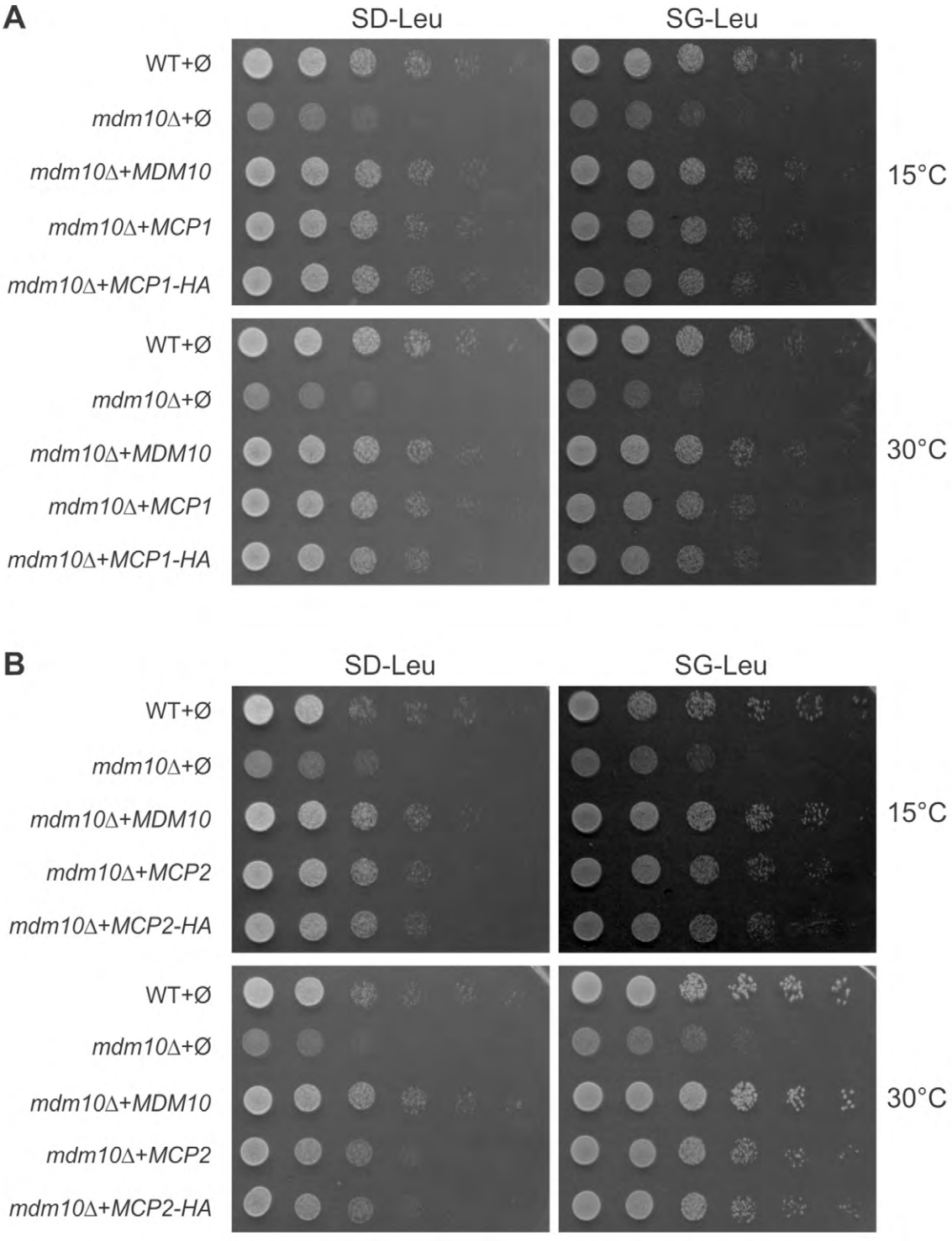


**Figure S5. Over-expression of C-terminally HA-tagged Mcp1 (A) and Mcp2 (B) rescues the *mdm10*Δ growth phenotype.** Overnight cultures of the indicated strains were diluted in selective glycerol-containing medium and grown to logarithmic phase. Serial 5-fold dilutions were spotted onto plates with selective medium containing either glucose (SD-Leu) or glycerol (SG-Leu) and incubated at either 30°C or 15°C.

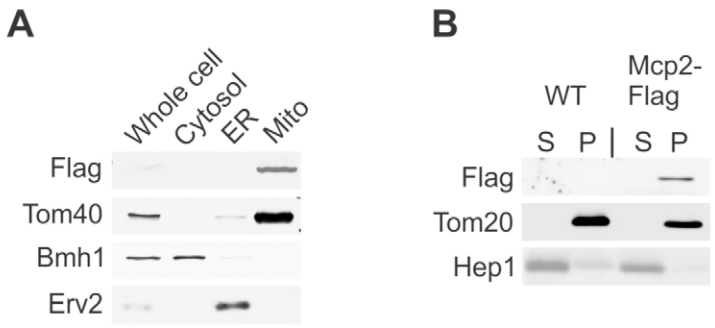


**Figure S6. Mcp2 is a mitochondrial membrane protein. (A)** Cells containing C-terminally Flag-tagged Mcp2 were subjected to subcellular fractionation. Whole cell lysate (Whole cell) and fractions corresponding to cytosol, light microsomal fraction (ER) and mitochondria (Mito) were analyzed by SDS-PAGE and immunodecoration with antibodies against Flag-tag, the mitochondrial protein Tom40, the ER protein Erv2 and a marker protein for the cytosol (Bmh1). **(B)** Mitochondria isolated from WT or cells expressing Mcp2-Flag were subjected to alkaline extraction. The supernatant (S) and pellet (P) fractions were analyzed by SDS-PAGE and immunodecoration with antibodies against Flag-tag, Tom20 (an integral MOM protein) and Hep1 (soluble matrix protein).

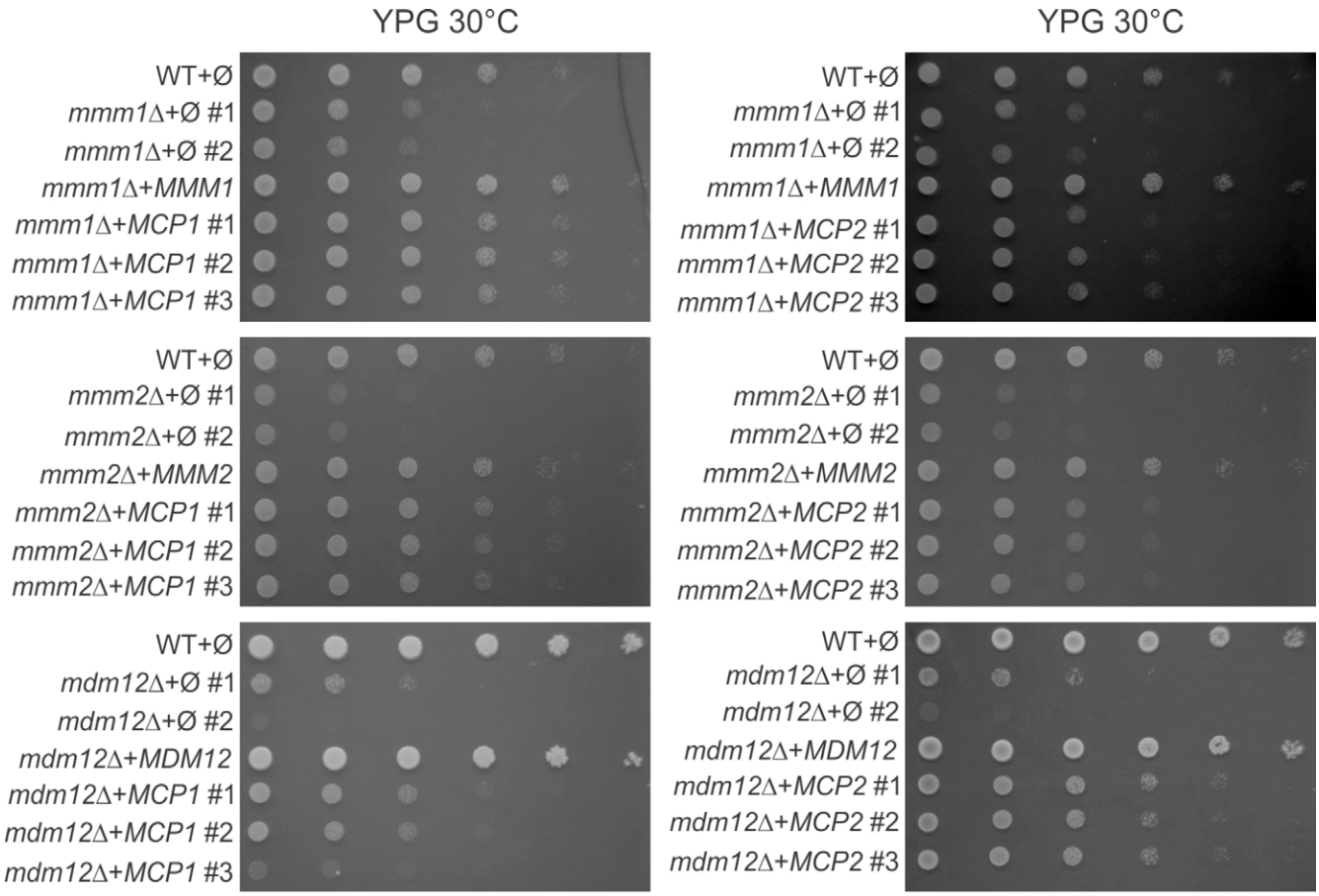


**Figure S7. Over-expression of Mcp1 and Mcp2 can suppress the growth phenotype of *mmm1*Δ, *mmm2*Δ *and mdm12*Δ cells.** Overnight cultures of the indicated strains were diluted in glycerol containing rich medium and grown to logarithmic phase. Serial 5-fold dilutions were spotted onto YPG plates and cells were incubated at 30°C. Two independent transformants carrying the empty plamid (Ø, #1-2) and three independent transformants harboring the over-expression plasmid (#1-3) were analysed.

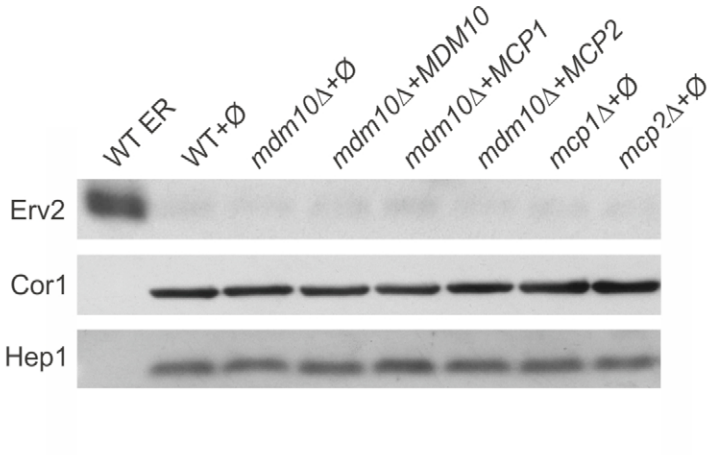


**Figure S8. ER contamination levels of purified mitochondria.** The same amount (30 µg) of gradient-purified mitochondria from the indicated yeast strains and of an ER fraction from wild-type cells (WT ER) were analysed by SDS-PAGE and immunodecoration with antibodies against the ER protein Erv2 and the mitochondrial proteins Cor1 and Hep1.

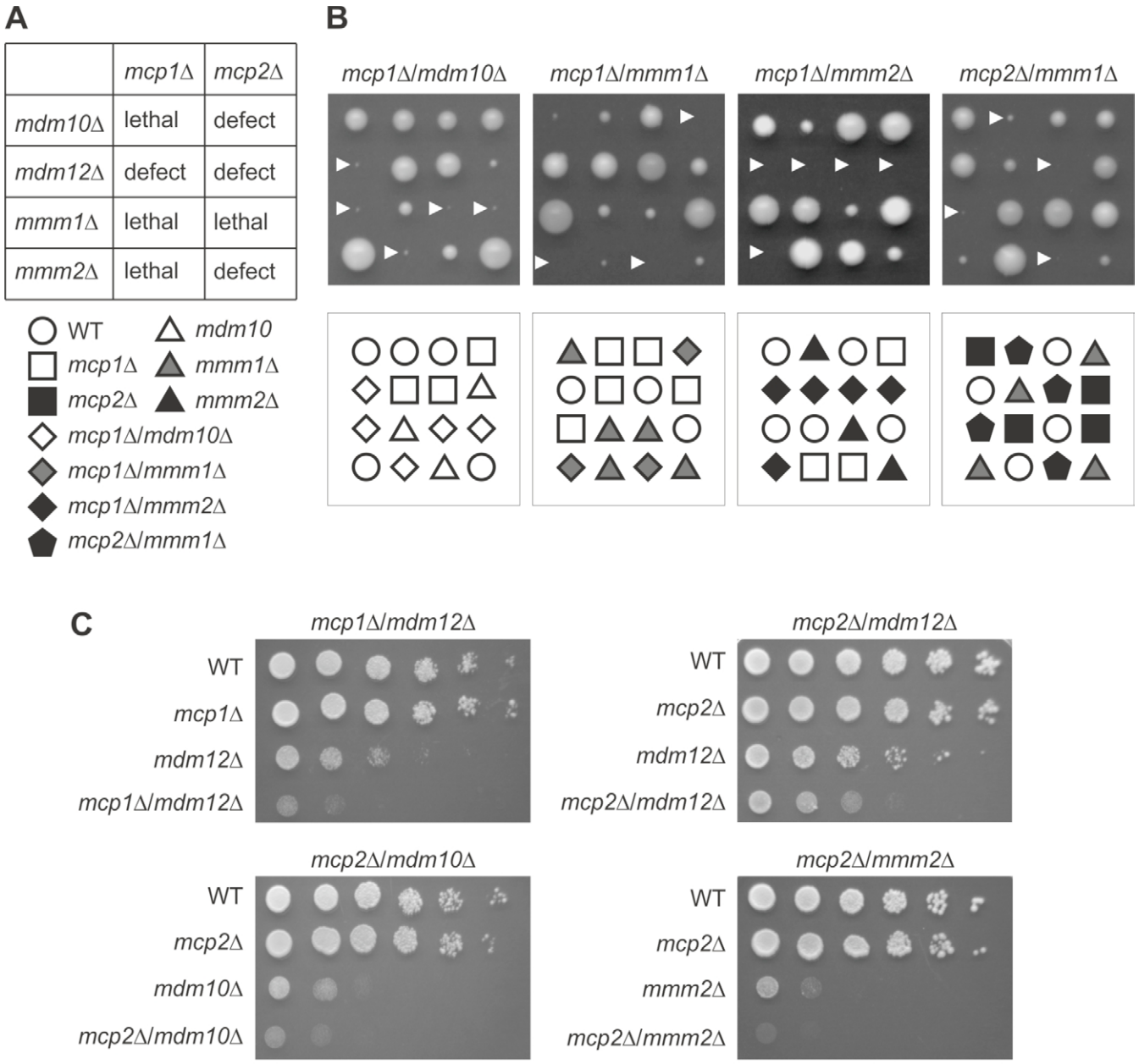


**Figure S9. Genetic interactions of *mcp1*Δ and *mcp2*Δ with deletions of genes of the ERMES complex. (A)** Summary of the observed synthetic effects of *mcp1*Δ or *mcp2*Δ in combination with *mdm10*Δ, *mdm12*Δ, *mmm1*Δ or *mmm2*Δ. **(B)** Synthetic lethality of *mcp1*Δ in combination with *mdm10*Δ, *mmm1*Δ or *mmm2*Δ and *mcp2*Δ with *mmm1*Δ identified by tetrad analysis. The genetic identity of the various colonies is depicted in a symbol key. **(C)** Synthetic growth defects of *mcp1*Δ in combination with *mdm12*Δ and *mcp2*Δ with *mdm10*Δ, *mdm12*Δ or *mmm2*Δ were analysed by drop dilution assay on rich medium containing glucose at 37°C after 3 days.

**Table S1. Amount of phospholipids [mol% ± s.d.] and ergosterol/phospholipid ratio [ERG/PL ± SD] of mitochondria isolated from the indicated strains**

| | WT +pYX142 | *mdm10*Δ +pYX142 | *mdm10*Δ +MDM10 | *mdm10*Δ +MCP1 | *mdm10*Δ +MCP2 | *mcp1*Δ +pYX142 | *mcp2*Δ +pYX142 |
|---|---|---|---|---|---|---|---|
| PC | 17.06 ± 1.71 | 17.38 ± 2.67 | 16.20 ± 2.61 | 14.18 ± 2.09 | 13.56 ± 2.33 | 14.96 ± 3.14 | 17.70 ± 3.05 |
| PE | 43.06 ± 4.37 | 30.26 ± 0.93 | 46.06 ± 5.98 | 45.59 ± 5.99 | 37.13 ± 4.38 | 46.04 ± 4.46 | 41. 25 ± 2.38 |
| PI | 11.02 ± 2.85 | 10.58 ± 2.51 | 7.73 ± 2.28 | 8.44 ± 1.69 | 11.16 ± 3.09 | 9.95 ± 2.07 | 9.73 ± 1.30 |
| PS | 3.68 ± 1.21 | 7.57 ± 1.84 | 3.65 ± 1.54 | 4.17 ± 1.57 | 5.98 ± 2.33 | 3.16 ± 0.87 | 3.47 ± 0.96 |
| PG | 0.67 ± 0.23 | 0.85 ± 0.36 | 0.96 ± 0.35 | 0.91 ± 0.42 | 0.61 ± 0.27 | 0.83 ± 0.20 | 0.93 ± 0.31 |
| CL | 10.94 ± 1.66 | 7.24 ± 2.49 | 10.82 ± 2.98 | 8.00 ± 1.81 | 8.43 ± 2.47 | 11.28 ± 1.58 | 10.59 ± 1.74 |
| ERG | 13.55 ± 1.48 | 26.13 ± 3.98 | 14.58 ± 2.74 | 18.72 ± 3.16 | 23.13 ± 3.28 | 13.78 ± 4.11 | 16.33 ± 1.62 |
| Ergosterol/phospholipid ratio | | | | | | | |
| ERG/PL | 0.16 ± 0.02 | 0.36 ± 0.07 | 0.17 ± 0.04 | 0.23 ± 0.05 | 0.30 ± 0.05 | 0.16 ± 0.06 | 0.20 ± 0.02 |

**Table S2. Relative amount of different species of the single phospholipids**

Phosphatidylcholine

| >0.2% | mean | | | | | | |
|---|---|---|---|---|---|---|---|
| | WT + pYX142 | *mdm10*Δ + pYX142 | *mdm10*Δ + *MDM10* | *mdm10*Δ + *MCP1* | *mdm10*Δ + *MCP2* | *mcp1*Δ + pYX142 | *mcp2*Δ + pYX142 |
| PC 28:1 | 1.03 | 0.40 | 0.80 | 0.90 | 0.93 | 1.29 | 0.99 |
| PC 30:2 | 0.43 | 0.26 | 0.57 | 0.48 | 0.35 | 0.52 | 0.32 |
| PC 30:1 | 1.94 | 1.44 | 1.97 | 1.99 | 1.71 | 2.57 | 2.16 |
| PC 30:0 | 0.24 | 0.05 | 0.19 | 0.20 | 0.23 | 0.31 | 0.28 |
| PC 32:2 | 27.79 | 27.73 | 30.30 | 27.86 | 24.05 | 27.13 | 28.06 |
| PC 32:1 | 12.49 | 9.42 | 12.47 | 12.36 | 11.74 | 14.49 | 14.28 |
| PC 34:2 | 35.53 | 41.46 | 34.25 | 35.68 | 38.12 | 32.47 | 33.23 |
| PC 34:1 | 11.61 | 9.48 | 10.96 | 10.89 | 12.17 | 12.56 | 12.43 |
| PC 36:2 | 5.15 | 6.42 | 5.01 | 5.69 | 6.49 | 4.85 | 4.52 |
| PC 36:1 | 3.32 | 2.99 | 2.92 | 3.25 | 3.61 | 3.29 | 3.19 |
| PC 36:0 | 0.16 | 0.12 | 0.20 | 0.20 | 0.15 | 0.16 | 0.19 |
| PC 38:0 | 0.24 | 0.17 | 0.29 | 0.40 | 0.38 | 0.28 | 0.26 |

| | Standard deviation | | | | | | |
|---|---|---|---|---|---|---|---|
| | WT + pYX142 | *mdm10*Δ + pYX142 | *mdm10*Δ + *MDM10* | *mdm10*Δ + *MCP1* | *mdm10*Δ + *MCP2* | *mcp1*Δ + pYX142 | *mcp2*Δ + pYX142 |
| PC 28:1 | 0.21 | 0.04 | 0.21 | 0.43 | 0.08 | 0.16 | 0.12 |
| PC 30:2 | 0.05 | 0.08 | 0.27 | 0.09 | 0.10 | 0.14 | 0.05 |
| PC 30:1 | 0.01 | 0.02 | 0.36 | 0.35 | 0.11 | 0.44 | 0.17 |
| PC 30:0 | 0.02 | 0.07 | 0.06 | 0.04 | 0.07 | 0.07 | 0.08 |
| PC 32:2 | 0.11 | 2.61 | 6.19 | 2.06 | 2.41 | 4.32 | 4.09 |
| PC 32:1 | 1.31 | 2.49 | 6.01 | 4.08 | 2.43 | 1.14 | 2.34 |
| PC 34:2 | 1.20 | 2.01 | 5.42 | 4.62 | 2.11 | 0.57 | 0.55 |
| PC 34:1 | 0.20 | 1.97 | 4.84 | 2.89 | 2.32 | 2.06 | 2.61 |
| PC 36:2 | 0.15 | 0.07 | 0.38 | 1.10 | 0.33 | 1.23 | 0.13 |
| PC 36:1 | 0.08 | 0.52 | 0.82 | 0.24 | 0.24 | 0.08 | 0.18 |
| PC 36:0 | 0.03 | 0.17 | 0.00 | 0.04 | 0.03 | 0.11 | 0.03 |
| PC 38:0 | 0.09 | 0.00 | 0.07 | 0.07 | 0.06 | 0.20 | 0.14 |

Phosphatidylethanolamine

| >0.5% | Mean | | | | | | |
|---|---|---|---|---|---|---|---|
| | WT + pYX142 | *mdm10*Δ + pYX142 | *mdm10*Δ + *MDM10* | *mdm10*Δ + *MCP1* | *mdm10*Δ + *MCP2* | *mcp1*Δ + pYX142 | *mcp2*Δ + pYX142 |
| PE 32:2 | 21.25 | 21.52 | 21.80 | 23.64 | 23.43 | 23.46 | 24.35 |
| PE 32:1 | 7.26 | 3.29 | 9.06 | 6.01 | 4.33 | 8.68 | 7.60 |
| PE 34:2 | 56.13 | 61.69 | 51.66 | 56.75 | 60.88 | 51.22 | 52.43 |
| PE 34:1 | 4.89 | 2.98 | 6.84 | 4.28 | 3.53 | 5.90 | 4.73 |
| PE 36:2 | 9.04 | 9.55 | 9.07 | 8.17 | 6.78 | 9.18 | 9.45 |

| | Standard deviation | | | | | | |
|---|---|---|---|---|---|---|---|
| | WT + pYX142 | *mdm10*Δ + pYX142 | *mdm10*Δ + *MDM10* | *mdm10*Δ + *MCP1* | *mdm10*Δ + *MCP2* | *mcp1*Δ + pYX142 | *mcp2*Δ + pYX142 |
| PE 32:2 | 0.26 | 3.55 | 4.11 | 2.29 | 0.15 | 0.28 | 1.38 |
| PE 32:1 | 0.52 | 0.01 | 2.07 | 0.17 | 0.22 | 1.06 | 0.07 |
| PE 34:2 | 1.15 | 0.33 | 2.51 | 0.71 | 0.30 | 1.80 | 0.21 |
| PE 34:1 | 0.55 | 0.79 | 3.05 | 0.71 | 0.01 | 1.14 | 0.20 |
| PE 36:2 | 1.17 | 3.04 | 0.30 | 0.09 | 0.14 | 2.21 | 0.24 |

Phosphatidylserine

| >0,5% | Mean | | | | | | |
|---|---|---|---|---|---|---|---|
| | WT + pYX142 | *mdm10*Δ + pYX142 | *mdm10*Δ + *MDM10* | *mdm10*Δ + *MCP1* | *mdm10*Δ + *MCP2* | *mcp1*Δ + pYX142 | *mcp2*Δ + pYX142 |
| PS 32:2 | 9.08 | 9.94 | 7.59 | 10.21 | 11.09 | 10.78 | 11.21 |
| PS 32:1 | 9.57 | 5.47 | 9.81 | 8.90 | 8.01 | 11.04 | 10.48 |
| PS 34:2 | 56.81 | 64.39 | 50.72 | 57.22 | 57.35 | 52.06 | 54.78 |
| PS 34:1 | 21.46 | 17.53 | 28.33 | 20.11 | 20.03 | 21.99 | 20.57 |
| PS 36:2 | 0.60 | 1.13 | 1.08 | 0.81 | 1.19 | 1.18 | 0.65 |
| PS 36:1 | 0.39 | 0.26 | 0.35 | 0.74 | 0.62 | 0.28 | 0.62 |

| | Standard deviation | | | | | | |
|---|---|---|---|---|---|---|---|
| | WT + pYX142 | *mdm10*Δ + pYX142 | *mdm10*Δ + *MDM10* | *mdm10*Δ + *MCP1* | *mdm10*Δ + *MCP2* | *mcp1*Δ + pYX142 | *mcp2*Δ + pYX142 |
| PS 32:2 | 1.20 | 3.29 | 2.38 | 0.05 | 1.44 | 0.66 | 3.87 |
| PS 32:1 | 2.16 | 1.48 | 6.23 | 1.36 | 0.18 | 2.92 | 3.96 |
| PS 34:2 | 8.03 | 4.49 | 17.22 | 7.21 | 2.02 | 10.29 | 11.87 |
| PS 34:1 | 0.90 | 2.08 | 9.66 | 2.18 | 0.47 | 4.30 | 8.22 |
| PS 36:2 | 0.51 | 0.36 | 0.21 | 0.41 | 0.05 | 0.45 | 0.47 |
| PS 36:1 | 0.31 | 0.37 | 0.49 | 0.47 | 0.34 | 0.39 | 0.68 |

Cardiolipin

| >1% | Mean | | | | | | |
|---|---|---|---|---|---|---|---|
| | WT + pYX142 | *mdm10*Δ + pYX142 | *mdm10*Δ + *MDM10* | *mdm10*Δ + *MCP1* | *mdm10*Δ + *MCP2* | *mcp1*Δ + pYX142 | *mcp2*Δ + pYX142 |
| CL 64:4 | 2.08 | 2.15 | 1.83 | 1.93 | 1.98 | 2.59 | 2.33 |
| CL 64:3 | 1.83 | 2.05 | 1.73 | 1.75 | 1.75 | 2.05 | 1.79 |
| CL 64:2 | 1.06 | 1.16 | 1.16 | 1.19 | 1.13 | 1.25 | 1.02 |
| CL 66:7 | 1.48 | 1.61 | 1.45 | 1.51 | 1.59 | 1.73 | 1.54 |
| CL 66:6 | 1.21 | 1.27 | 1.03 | 1.12 | 1.21 | 1.25 | 1.08 |
| CL 66:5 | 1.01 | 1.09 | 0.95 | 1.00 | 1.10 | 1.17 | 0.97 |
| CL 66:4 | 7.10 | 6.97 | 6.24 | 6.13 | 6.47 | 8.75 | 8.31 |
| CL 66:3 | 4.89 | 5.71 | 5.28 | 5.26 | 5.19 | 5.66 | 5.07 |
| CL 66:2 | 3.47 | 3.70 | 4.12 | 3.72 | 3.32 | 3.80 | 3.37 |
| CL 66:1 | 1.07 | 1.03 | 1.36 | 1.23 | 1.32 | 1.35 | 1.12 |
| CL 68:7 | 2.67 | 2.48 | 2.14 | 2.36 | 2.50 | 2.62 | 2.58 |
| CL 68:6 | 2.10 | 2.21 | 1.80 | 2.14 | 2.06 | 1.92 | 1.82 |
| CL 68:5 | 1.69 | 1.67 | 1.82 | 1.80 | 1.72 | 1.61 | 1.55 |
| CL 68:4 | 8.35 | 7.36 | 7.16 | 6.79 | 7.25 | 10.24 | 9.91 |
| CL 68:3 | 10.57 | 11.24 | 11.35 | 11.78 | 11.54 | 10.42 | 10.72 |
| CL 68:2 | 5.74 | 5.29 | 7.19 | 5.89 | 5.35 | 5.55 | 5.27 |
| CL 70:7 | 3.15 | 2.71 | 2.33 | 2.53 | 2.73 | 2.83 | 3.03 |
| CL 70:6 | 4.81 | 4.93 | 4.27 | 5.30 | 5.01 | 3.41 | 4.03 |
| CL 70:5 | 2.71 | 2.47 | 3.15 | 2.84 | 2.64 | 2.16 | 2.29 |
| CL 70:4 | 5.46 | 4.58 | 4.64 | 4.25 | 4.80 | 6.56 | 6.62 |
| CL 70:3 | 11.16 | 12.05 | 12.02 | 13.12 | 12.83 | 9.27 | 10.57 |
| CL 70:2 | 4.14 | 3.89 | 5.13 | 4.21 | 4.24 | 3.66 | 3.78 |
| CL 72:7 | 1.36 | 1.26 | 1.03 | 1.08 | 1.23 | 1.27 | 1.34 |
| CL 72:6 | 3.66 | 3.88 | 3.17 | 3.89 | 3.88 | 2.13 | 2.67 |
| CL 72:5 | 1.37 | 1.27 | 1.63 | 1.43 | 1.44 | 1.08 | 1.15 |
| CL 72:4 | 1.26 | 1.23 | 1.17 | 1.02 | 1.21 | 1.55 | 1.55 |
| CL 72:3 | 3.15 | 3.40 | 3.59 | 3.38 | 3.06 | 2.61 | 3.14 |

| | Standard deviation | | | | | | |
|---|---|---|---|---|---|---|---|
| | WT + pYX142 | *mdm10*Δ + pYX142 | *mdm10*Δ + *MDM10* | *mdm10*Δ + *MCP1* | *mdm10*Δ + *MCP2* | *mcp1*Δ + pYX142 | *mcp2*Δ + pYX142 |
| CL 64:4 | 0.00 | 0.01 | 0.13 | 0.16 | 0.63 | 0.10 | 0.49 |
| CL 64:3 | 0.40 | 0.29 | 0.07 | 0.16 | 0.16 | 0.04 | 0.02 |
| CL 64:2 | 0.35 | 0.19 | 0.24 | 0.42 | 0.00 | 0.01 | 0.15 |
| CL 66:7 | 0.45 | 0.45 | 0.40 | 0.24 | 0.45 | 1.16 | 0.42 |
| CL 66:6 | 0.39 | 0.46 | 0.37 | 0.39 | 0.48 | 0.91 | 0.45 |
| CL 66:5 | 0.19 | 0.26 | 0.26 | 0.13 | 0.31 | 0.78 | 0.28 |
| CL 66:4 | 0.62 | 1.07 | 0.85 | 0.61 | 1.74 | 0.95 | 1.07 |
| CL 66:3 | 1.34 | 1.30 | 1.24 | 1.25 | 0.30 | 0.92 | 0.64 |

| | | | | | | | |
|---|---|---|---|---|---|---|---|
| CL 66:2 | 1.32 | 1.43 | 0.95 | 1.57 | 0.21 | 0.36 | 0.73 |
| CL 66:1 | 0.02 | 0.17 | 0.16 | 0.18 | 0.04 | 0.42 | 0.01 |
| CL 68:7 | 0.61 | 0.23 | 0.18 | 0.47 | 0.66 | 0.90 | 0.67 |
| CL 68:6 | 0.41 | 0.64 | 0.19 | 0.27 | 0.44 | 0.98 | 0.41 |
| CL 68:5 | 0.31 | 0.30 | 0.34 | 0.11 | 0.26 | 0.90 | 0.14 |
| CL 68:4 | 1.51 | 1.63 | 1.44 | 0.62 | 1.31 | 3.17 | 0.44 |
| CL 68:3 | 1.73 | 0.88 | 2.11 | 2.06 | 2.42 | 2.40 | 1.85 |
| CL 68:2 | 1.33 | 1.87 | 0.42 | 1.53 | 1.17 | 0.48 | 1.08 |
| CL 70:7 | 0.59 | 0.21 | 0.21 | 0.73 | 0.86 | 0.80 | 0.78 |
| CL 70:6 | 1.64 | 2.12 | 0.46 | 0.69 | 0.15 | 1.48 | 0.24 |
| CL 70:5 | 0.91 | 0.59 | 1.26 | 0.64 | 0.25 | 1.26 | 0.36 |
| CL 70:4 | 1.02 | 1.01 | 0.94 | 0.37 | 0.51 | 2.50 | 0.19 |
| CL 70:3 | 0.66 | 1.50 | 0.16 | 0.56 | 3.23 | 1.40 | 1.40 |
| CL 70:2 | 0.10 | 0.16 | 1.62 | 0.01 | 0.76 | 0.34 | 0.40 |
| CL 72:7 | 0.33 | 0.14 | 0.18 | 0.34 | 0.40 | 0.31 | 0.31 |
| CL 72:6 | 1.76 | 1.84 | 0.76 | 0.91 | 0.40 | 0.79 | 0.09 |
| CL 72:5 | 0.67 | 0.51 | 0.98 | 0.61 | 0.08 | 0.74 | 0.24 |
| CL 72:4 | 0.07 | 0.21 | 0.07 | 0.10 | 0.15 | 0.40 | 0.06 |
| CL 72:3 | 0.24 | 0.22 | 0.64 | 0.08 | 0.53 | 0.30 | 0.40 |

Phosphatidylinositol

| Mean | | | | | | | |
|---|---|---|---|---|---|---|---|
| | WT + pYX142 | *mdm10*Δ + pYX142 | *mdm10*Δ + *MDM10* | *mdm10*Δ + *MCP1* | *mdm10*Δ + *MCP2* | *mcp1*Δ + pYX142 | *mcp2*Δ + pYX142 |
| PI 32:2 | 5.11 | 4.88 | 7.05 | 5.76 | 5.29 | 5.82 | 5.61 |
| PI 32:1 | 24.42 | 17.71 | 23.77 | 21.37 | 19.27 | 24.24 | 24.30 |
| PI 34:2 | 11.67 | 15.00 | 11.44 | 13.76 | 12.57 | 10.44 | 10.12 |
| PI 34:1 | 44.09 | 40.17 | 39.74 | 42.32 | 44.64 | 43.91 | 44.19 |
| PI 36:1 | 14.18 | 20.75 | 17.38 | 16.15 | 16.99 | 14.97 | 15.13 |

| Standard deviation | | | | | | | |
|---|---|---|---|---|---|---|---|
| | WT + pYX142 | *mdm10*Δ + pYX142 | *mdm10*Δ + *MDM10* | *mdm10*Δ + *MCP1* | *mdm10*Δ + *MCP2* | *mcp1*Δ + pYX142 | *mcp2*Δ + pYX142 |
| PI 32:2 | 1.16 | 2.90 | 0.03 | 0.54 | 0.91 | 0.69 | 0.53 |
| PI 32:1 | 0.80 | 0.85 | 5.50 | 0.63 | 0.31 | 2.69 | 0.90 |
| PI 34:2 | 0.35 | 0.85 | 3.94 | 0.58 | 1.93 | 1.20 | 2.99 |
| PI 34:1 | 0.08 | 3.20 | 2.81 | 1.42 | 0.92 | 1.23 | 0.73 |
| PI 36:1 | 1.37 | 6.16 | 2.15 | 1.67 | 1.99 | 0.56 | 2.29 |

Phosphatidylglycerol

| Mean | | | | | | | |
|---|---|---|---|---|---|---|---|
| | WT + pYX142 | *mdm10*Δ + pYX142 | *mdm10*Δ + *MDM10* | *mdm10*Δ + *MCP1* | *mdm10*Δ + *MCP2* | *mcp1*Δ + pYX142 | *mcp2*Δ + pYX142 |
| PG 32:2 | 5.77 | 7.87 | 6.75 | 7.55 | 8.09 | 8.05 | 6.76 |
| PG 32:1 | 23.37 | 21.57 | 24.36 | 26.59 | 21.70 | 23.03 | 25.66 |
| PG 34:2 | 15.04 | 20.64 | 14.19 | 13.85 | 17.50 | 16.01 | 14.51 |
| PG 34:1 | 46.58 | 41.13 | 46.17 | 43.31 | 37.09 | 41.74 | 45.99 |
| PG 36:2 | 2.13 | 2.42 | 2.10 | 1.75 | 3.77 | 2.69 | 1.34 |
| PG 36:1 | 3.67 | 2.33 | 3.75 | 3.11 | 5.87 | 2.58 | 1.65 |

| Standard deviation | | | | | | | |
|---|---|---|---|---|---|---|---|
| | WT + pYX142 | *mdm10*Δ + pYX142 | *mdm10*Δ + *MDM10* | *mdm10*Δ + *MCP1* | *mdm10*Δ + *MCP2* | *mcp1*Δ + pYX142 | *mcp2*Δ + pYX142 |
| PG 32:2 | 3.10 | 3.14 | 5.36 | 0.63 | 0.99 | 1.72 | 1.55 |
| PG 32:1 | 0.59 | 0.92 | 5.17 | 4.93 | 2.39 | 2.85 | 1.52 |
| PG 34:2 | 1.41 | 5.93 | 8.46 | 4.24 | 2.25 | 2.89 | 0.86 |
| PG 34:1 | 12.61 | 3.56 | 13.69 | 6.15 | 2.54 | 5.83 | 6.51 |
| PG 36:2 | 1.97 | 1.01 | 0.99 | 1.39 | 0.46 | 0.90 | 1.23 |
| PG 36:1 | 0.67 | 1.75 | 0.25 | 0.78 | 0.48 | 1.32 | 1.31 |

**Table S3. Sequences of primers used in this study**

| | |
|---|---|
| **Primers for deletion by gene-targeting** | |
| mdm10fwd | 5' AAA TAT ACG TTA GGA AAA AGA CAC GAA CAG AGA AGA CCG ATC TTG *CGT ACG CTG CAG GTC GAC* 3' |
| mdm10rev | 5' ATT TTT TAA CCT GTA TAT TAA AAC CTT TAT TTT ATT TCA CAT TAC *ATC GAT GAA TTC GAG CTC G* 3' |
| mcp1fwd | 5' ATT ACT AGG GCA TAT ACC AGT TAG CCC AGA GTT TTG TTT ATT ACG *CGT ACG CTG CAG GTC GAC* 3' |
| mcp1rev | 5' GAA TTG TCG CAA ATT AAT AGC TTC ACA CTA CTC CCA CAA GGA TTC *ATC GAT GAA TTC GAG CTC G* 3' |
| mcp2fwd | 5' GAG CAA GAT TAT AGT TGA ATG TTT CTT ATT CGG TGT TGA TAG TAG *CGT ACG CTG CAG GTC GAC* 3' |
| mcp2rev | 5' TAT AAT TTT ACG TAT ATA TTT ACA AGT AGA AAG AAC GCT AAC GAT *ATC GAT GAA TTC GAG CTC G* 3' |
| **Primers for introducing open reading frames into pYX plasmids** | |
| pYXmdm10s | 5'GGG *CCA TGG* CCA TGC TAC CCT ATA TGG ACC AA 3' |
| pYXmdm10a1 | 5´ GGG *CCC GGG* TCA TGT GGA GTA CTG GAA TTG 3' |
| pYXmdm10a2 | 5' GGG *CCC GGG* TGT GGA GTA CTG GAA TTG TAT 3' (omitting the stop codon for a plasmid-borne HA-Tag) |
| pYXmmm1s | 5' GGG *CCA TGG* CCA TGA CTG ATA GTG AGA ATG AAT C 3' |
| pYXmmm1a1 | 5' GGG *CCC GGG* TTA TAA CTC TGT AGG CTT TTC TT 3' |
| pYXmmm2s | 5' GGG *CCA TGG* CCA TGT CAT TTA GAT TCA ACG AAG C 3' |
| pYXmmm2a1 | 5' GGG *AAG CTT* TTA ATG ATA TGG TGG GGG GC 3' |
| pYXmdm12s | 5' GGG *GAA TTC* ATG TCT TTT GAT ATT AAT TGG AGT 3' |
| pYXmdm12a1 | 5' GGG *AAG CTT* TTA CTC ATC ACC ATC GTT GAA A 3' |
| pYXmcp1s | 5' GGG *GGA TCC* CAT AAA GTT GCA TGA AGT GCC T 3' |
| pYXmcp1a1 | 5' GGG *AAG CTT* CTA ATT CAC GTG CAA CAG CAA 3' |
| pYXmcp1a2 | 5' GGG *AAG CTT* ATT CAC GTG CAA CAG CAA CC 3' (omitting the stop codon for a plasmid-borne HA-Tag) |
| pYXmcp2s | 5' GGG *CCA TGG* CCA TGA TGA CCA AAG CTT TTT TTA A 3' |
| pYXmcp2a1 | 5' GGG *CCC GGG* TTA AGA TGA CAA CCA AGT CTT C 3' |
| pYXmcp2a2 | 5' GGG *CCC GGG* AGA TGA CAA CCA AGT CTT CGG 3' (omitting the stop codon for a plasmid-borne HA-Tag) |

| **Primers for FLAG-tagging by gene-targeting** | |
|---|---|
| Flagmcp1fwd | 5’ TTC GAA AGC ATT TTC AAA AAG ATC CGG TTG CTG TTG CAC GTG AAT *ACT AGT GGA TCC CCC GGG* 3’ |
| Flagmcp1rev | 5’ GAA TTG TCG CAA ATT AAT AGC TTC ACA CTA CTC CCA CAA GGA TTC *ATC GAT GAA TTC GAG CTC G* 3’ |
| Flagmcp1fwd | 5’ GTG TTG TGG TGG AAA AAA TTT ATT CCG AAG ACT TGG TTG TCA TCT *ACT AGT GGA TCC CCC GGG* 3’ |
| Flagmcp1rev | 5’ TAT AAT TTT ACG TAT ATA TTT ACA AGT AGA AAG AAC GCT AAC GAT *ATC GAT GAA TTC GAG CTC G* 3’ |

The parts of sequences of primers used for amplification of gene-targeting cassettes that are homologues to the template plasmid and restriction enzyme recognition sites used for cloning are in italics.